JOURNAL OF PROTEOMICS 76 (2012) 220–238

Available online at www.sciencedirect.com

SciVerse ScienceDirect

www.elsevier.com/locate/jprot

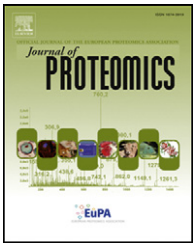

Effects of pre-storage leukoreduction on stored red blood cells signaling: A time-course evaluation from shape to proteome☆

Marianna H. Antonelou[a], *Vassilis L. Tzounakas*[a], *Athanassios D. Velentzas*[a], *Konstantinos E. Stamoulis*[b], *Anastasios G. Kriebardis*[c], *Issidora S. Papassideri*[a,*]

[a]*Department of Cell Biology and Biophysics, Faculty of Biology, NKUA, Greece*
[b]*Blood Transfusion Center, Nikea, Piraeus, Greece*
[c]*Laboratory of Hematology and Transfusion Medicine, Department of Medical Laboratories, Faculty of Health and Caring Professions, Technological and Educational Institute of Athens, Greece*

ARTICLE INFO

Available online 13 July 2012

Keywords:
Storage lesion
Red cell aging
Pre-storage leukoreduction
Membrane proteome
Oxidative stress
Calcium accumulation

ABSTRACT

The introduction of pre-storage leukoreduction in the preparation of standard RBCs intended for transfusion provided significant improvement in the quality of labile products and their post transfusion viability and effects, although the literature data are controversial. To elucidate the issue of the probable leukoreduction effects on RBCs storage lesion, we evaluated various storage quality measures in RBCs stored in either leukoreduced (L) or non-leukoreduced (N) units, with emphasis to senescence and oxidative stress associated modifications. Our data suggest that the residual leukocytes/platelets of the labile products represent a stressful storage factor, countering the structural and functional integrity of stored RBCs. Hemolysis, irreversible echinocytosis, microvesiculation, removal signaling, ROS/calcium accumulation, band 3-related senescence modifications, membrane proteome stress biomarkers as well as emergence of a senescence phenotype in young RBCs that is disproportionate to their age, are all encountered more or mostly in N-RBCs compared to the L-RBCs, either for a part or for the whole of the storage period. The partial, yet significant, alleviation of so many storage-related manifestations in the L-RBCs compared to the N-RBCs, is presented for the first time and provides a rational mechanistic interpretation of the improved storage quality and transfusions observed by the introduction of pre-storage leukoreduction.

This article is part of a Special Issue entitled: Integrated omics.

Abbreviations: BS3, bis-sulfosuccinimidyl-suberate; CSLM, confocal laser scanning microscopy; CPD, citrate-phosphate-dextrose; CMH2DCFDA, 5-(and-6)-chloromethyl-2′,7′-dichloro-dihydro-fluorescein diacetate, acetyl ester; DCF, dichlorofluorescein; Fluo-4AM, fluorescent calcium indicator Fluo-4; Hb, hemoglobin; HCT, hematocrit; L, leukoreduced; MCH, mean cell Hb; MCHC, mean cell Hb concentration; MCV, mean cell volume; N, non-leukoreduced; NEM, N-ethylmaleimide; NS, non-stored; PCI, proteome carbonylation index; PS, phosphatidylserine; Prx2, peroxiredoxin 2; RBCs, red blood cells; RDW, red cell distribution width; SAGM, saline-adenine-glucose-mannitol; S-RBCs, high-density fractions of RBCs enriched in senescent-RBCs; t-BHP, tert-butyl hydroperoxide; Y-RBCs, low-density fractions of RBCs enriched in young RBCs.

☆ This article is part of a Special Issue entitled: Integrated omics.

* *Corresponding author at:* Department of Cell Biology and Biophysics, Faculty of Biology, NKUA, Panepistimiopolis, Athens 15784, Greece. Tel.: +30 210 7274546; fax: +30 210 7274742.
E-mail address: ipapasid@biol.uoa.gr (I.S. Papassideri).

1874-3919/$ – see front matter © 2012 Elsevier B.V. All rights reserved.
doi:10.1016/j.jprot.2012.06.032

1. Introduction

Effective *ex vivo* storage of red blood cells (RBCs) is an essential requirement for medical practice. Stored RBCs undergo a series of time-dependent – yet early enough recognizable – physiological, structural and biochemical alterations, which are only reversible to some extent [1]. In the RBC storage lesion context, physiologically important disturbances in energy metabolism, rheological properties (shape, deformability, aggregability, intracellular viscosity), oxidation/carbonylation stress and finally, in cellular aging process have been widely characterized [1,2]. Altered membrane surface and cytoskeleton contribute to the RBCs damage and clearance [3,4]. Although the clinical importance of the RBCs storage lesion is poorly understood, some of the irreversible deteriorations of the stored RBCs, like hemolysis, potassium release and microvesicles accumulation, are associated with reduced post-transfusion survival/efficacy and increased risk of adverse reactions in the recipients [5,6].

The currently used techniques for the preparation of standard RBCs products include the pre-storage filtration of blood to remove the contaminating donor leukocytes and platelets. Despite controversy among the randomized clinical trials on the beneficial or neutral effects of filtration [7,8], the introduction of pre-storage leukoreduction has provided significant improvement in transfusions by lowering the incidence of viruses transmission and the circumstantial, yet severe, untoward clinical effects (alloimmunization, immunosuppression, inflammatory responses etc.) that have been related to increased morbidity/mortality liability [5,9]. Moreover, the leukoreduction exhibits a beneficial effect on RBCs storage lesion, by improving both the hemolysis and the post-transfusion recovery of leukoreduced RBCs [9,10]. Activated, apoptotic or degenerated leukocytes could equally trigger adverse transfusion reactions and storage-associated damage, since they represent a source for bioactive factors, like oxygen free radicals, cytokines and enzymes [10,11]. However, pre-storage leukocyte reduction has not eliminated all the leukocyte-related responses [12] nor the biochemical and morphological changes that occur to RBCs as a consequence of aging and storage [13]. As a matter of fact, some authors claimed that there is but a modest improvement in post-infusion viability of leukoreduced RBCs vs. the non-leukoreduced ones [14]. Further on, a recent study suggested that the pre-storage filtration may aggravate blood storage lesions [15]. Finally, although leukoreduction has been assigned as a standard in the labile products making, today, approximately 20% of the transfusions in the United States [16] and much higher percentage of those performed in several European countries are still conservative, namely non-leukoreduced. Therefore, there is still a need for clarifying the probable effects of leukoreduction on storage lesion progression as well as on *in vivo* efficacy and adverse transfusion effects. Adequate inventory and understanding of RBCs storage lesion in relation to various storage strategies currently followed in clinical practice is probably the only way to mitigate the disturbances that render RBC transfusions dangerous or less effective.

This study aims at reporting experimental facts touching the effect of residual leukocytes in the progression of RBCs storage lesion under standard blood banking conditions, with emphasis to the senescence and oxidative stress associated molecular and cellular modifications. To this purpose, we evaluated a series of storage quality measures in RBCs stored in either leukoreduced (L) or non-leukoreduced (N) units. A careful standardization of sample harvesting, process and storage was set up in order to minimize the pre-analytical variations. Our hematological, structural, biochemical and proteomic data suggest that the residual leukocytes and platelets represent an additional stressful factor for the stored RBCs, affecting almost all RBCs removal signaling mechanisms and thus their structural and functional integrity. The partial, yet significant, alleviation of so many storage-related manifestations in L-RBCs compared to N-RBCs is presented for the first time and provides a rational mechanistic interpretation of the improved storage quality and transfusions observed after the introduction of pre-storage leukoreduction.

2. Materials and methods

2.1. *Material supplies*

Antibodies against band 3, spectrin, human IgGs and HRP-conjugated antibodies to goat IgGs, as well as protease inhibitor cocktails, phosphatase inhibitor cocktail 2, t-butyl hydroperoxide (t-BHP) alpha-cellulose, microcrystalline cellulose (type 50), N-ethylmaleimide (NEM), Percoll medium (d = 1.13 g/ml), Drabkin's reagent components and common chemicals and buffers were all obtained from Sigma–Aldrich (Munich, Germany). Electron microscopy grade glutaraldehyde solution was from Serva (Heidelberg, Germany). Antibodies against hemoglobin (Hb) and peroxiredoxin 2 (Prx2) were obtained from Europa Bioproducts (UK) and from Acris GmbH (Herford, Germany), respectively. Antibodies against CD47, clusterin, HSP70, calpain-1 (μ-calpain), cathepsin E and band 3 were from Santa Cruz Biotechnology (CA, USA). Anti-human CD59 and HRP-conjugated anti-rabbit IgG were from R&D Systems (MN, USA). mAbs against synexin (annexin VII) and flotillin-2 were obtained from BD Transduction Laboratories (CA, USA). Sodium orthovanadate and Syk inhibitors II and IV were from Calbiochem (Darmstadt, Germany). bis-sulfosuccinimidyl-suberate (BS3) crosslinker was from Thermo Scientific (Rockford, IL). Anti-phosphotyrosine (pTyr, clone PY20) mAb, MF membrane syringe driven filters and the Oxyblot® detection kit were obtained from Millipore (Temecula, CA). A-23187 ionophore and annexin-V-Fluos solution were from Roche Diagnostics (Burgdorf, Switzerland). 5-(and-6)-chloromethyl-2′,7′-dichloro-dihydro-fluorescein diacetate, acetyl ester (CMH2DCFDA) and fluorescent calcium indicator Fluo-4 (Fluo-4 AM) were from Invitrogen, Molecular Probes (Eugene, OR). HRP-conjugated antibodies to rabbit IgGs, ECL Western blot detection kit and Percoll solution (d = 1.131 g/ml) were from GE Healthcare (Buckinghamshire, UK). HRP-conjugated antibodies to mouse IgGs were from DakoCytomation (Glostrup, Denmark). Rabbit anti-human CD235a was from AbD Serotec (Oxford, UK). Bradford protein assay was obtained from Bio-Rad (Hercules, CA). Western lighting Plus ECL was from Perkin Elmer (CA, USA). mAb against stomatin and antiserums against proteins 4.1R and pallidin (band 4.2) were kindly provided by Prof. R. Prohaska (Institute of Medical

Biochemistry, University of Vienna, Austria) and Prof. J.Delaunay (Laboratoire d'Hématologie, d'Immunologie et de Cytogénétique, Hopital de Bicetre, Le Kremlin-Bicetre, France) respectively.

2.2. Study planning, subjects and RBCs storage in blood bank conditions

Venous blood of 12 eligible, young (22–42 years old) blood donors was used in the present study. Initially, packed RBCs from 8 different donors stored in citrate-phosphate-dextrose (CPD) (CPD)/saline-adenine-glucose-mannitol (SAGM) units with (L, n=4) or without (N, n=4) filter leukoreduction were studied. By preliminary hematological analysis any aberrations from the average hematological profile were excluded. In order to examine the influence of donor variation to the diversification observed between stored L- and N-RBCs, we prepared L-RBCs preparations from 4 additional donors (n=4) under the same storage conditions. After a rational period of time, the same donors donated blood to prepare N-RBCs units (n=4). That approach was considered more reliable compared to the usually engaged division of a unit into filtered and non-filtered components, because it allows analysis of cell components under original volume and blood banking conditions. The hematological and blood biochemical analysis performed after the second donation verified the presence of a stable, normal hematologic profile, while a strict standardization of all procedures, analytical protocols and methodologies followed (blood collection conditions, type of anticoagulant and additive solutions, time/temperature before processing, working and storage duration and temperature, sampling volumes and timing, needle-to-analysis time, freeze-thaw cycles for frozen membranes etc.) ensured minimal levels of pre-analytical and analytical variations among the different measurements. The study has been submitted and approved by the Research Bioethics and BioSecure Committee of the Faculty of Biology/NKUA. Investigations were carried out in accordance with the principles of the Declaration of Helsinki. Informed consent was obtained from all blood donors participating in this study.

Collection and processing of blood, as well as isolation, storage and sampling of packed RBCs under various conditions were performed as previously described [17]. Briefly, whole blood was collected in a CPD/SAGM triple blood bag system (Baxter, Rome, Italy), anticoagulated with 63 ml of CPD (2.63 g sodium citrate dihydrate, 0.30 g citric acid monohydrate, 2.55 g dextrose monohydrate, 0.222 g monobasic sodium biphosphate monohydrate) and passed through leukoreduction filters (only for the L-preparations) according to the manufacturer's instructions. In order to prepare fresh frozen plasma from the same donations (for transfusion purposes) the blood units were filter leukodepleted after 8 h hold-up time at room temperature. RBCs concentrates were prepared by centrifugation in an automated blood processing device (Compomat G4, Fresenius HemoCare) before 100 ml of SAGM solution (0.9 g dextrose monohydrate, 0.877 g sodium chloride, 0.0169 g adenine, 0.525 g D-mannitol) was added. Then RBCs were stored for 7 weeks at 2 to 6 °C. From the first 2–4 days of storage and weekly thereafter, a sample was collected from the stored units (5–20 μl for the microscopy and fluorometry experiments, 2.5–3.5 ml for the RBCs fractionation and membrane preparations and 60 ml for the vesicles preparation on day 17 of storage) by a sterile sampling device, after gentle mixing of the unit content. As controls, donor RBCs collected before the banking procedure as well as stored RBCs of days 0–4 were used. Differential leukocyte and RBC counts, hematocrit (HCT), Hb concentration and RBCs indexes (mean cell volume, MCV; mean cell Hb, MCH; mean cell Hb concentration, MCHC; RBC distribution width, RDW) were performed using an automatic blood cell counter (Sysmex K-4500, Roche). Residual leukocytes measurement post-filtration was performed manually by the Türk's solution method. Percentage hemolysis was determined by comparing the supernatant Hb to total Hb concentrations, using Drabkin's method [18,19]. The HCT of each sample was measured before assay using microhematocrit centrifuge.

2.3. Electron microscopy

For the morphological evaluation of RBCs by scanning electron microscopy, purified RBCs were fixed with 2% glutaraldehyde and post-fixed with 1% osmium tetroxide in 0.1 mol/L sodium cacodylate buffer, pH 7.4. Fixed cells were successively dehydrated in ascending ethanol series and allowed to settle on standard microscopic cover glasses. Finally, RBCs were coated with gold–palladium (Tousimis Samsputter-2a, Rockville, Maryland) before being examined in a microscope (Philips SEM515). Classification of cell transformations was achieved by using the standard criteria with minor modifications as previously described [20,21]. All spherocytic modifications of the stored cells (spherocytes, spheroechinocytes and spherostomatocytes) along with RBCs presented with degenerative shapes were assorted to the "irreversibly" transformed cells group, as previously suggested [22,23]. The percentage of discocytes and that of irreversible (see above) or reversible (all the other types of minor to severe shape modifications, e.g. echinocytes type III) was estimated by 3 independent individuals in "blind" electron micrographs containing at least 2000 cells from randomly chosen fields. Only the perfectly shaped discocytes have been included in the category "normal RBCs". Discocytes with even minor alterations in volume, surface or contour were characterized as reversibly changed cells.

2.4. PS externalization in stored RBCs

Detection of phosphatidylserine (PS) exposure was performed by confocal laser scanning microscopy (CSLM) analysis of RBCs labeled with annexin V that is a calcium-dependent, sensitive PS probe. 10^6 L- and N-RBCs stored for various periods in CPD-SAGM were incubated in a calcium-containing buffer (10 mmol/L Hepes/NaOH, pH 7.4, 140 mmol/L NaCl, 5 mmol/L $CaCl_2$) and labeled with the fluorescent Annexin-V-Fluos solution for 15 min at 20 °C in the dark, according to the manufacturer's recommendations. Examination was performed with CLSM (Digital Eclipse C1, Nikon, NY) using an excitation wavelength of 488 nm and detection in the range of 515–565 nm (green), with recordings at the same exposure times. As positive controls, we used N-ethylmaleimide- (inhibitor of aminophospholipid translocase) pre-treated cells, *in vitro* oxidized cells or cells loaded with calcium/ionophore A23187. As negative controls, non-stored RBCs from each donor as well as freshly donated blood were

used and were either free of signaling or they presented with extremely low percentage of PS-positive cells (<0.06%). The percentage of PS-positive RBCs in each sample was evaluated in triplicate assays, by counting 800 RBCs at least in randomly chosen fields.

2.5. Determination of intracellular ROS and calcium

ROS accumulation in stored RBCs was detected with the membrane-permeable, non-fluorescent and redox-sensitive probe 5-(and-6)-chloromethyl-2′,7′-dichloro-dihydro-fluorescein diacetate, acetyl ester (CM-H_2DCFDA) according to the manufacturer's guidelines with minor modifications as previously described [21]. CM-H_2DCFDA is de-esterified inside the cell. Oxidation of the de-esterified product by intracellular ROS yields the fluorescent DCF (dichlorofluorescein) product that can be quantified by fluorometry or flow cytometry. More specifically, isolated, leukocyte-depleted (by cellulose columns, see below) and thoroughly washed RBCs at 1% HCT (each sample in triplets) were loaded with 10 μmol/L CM-H_2DCFDA in PBS buffer for 30 min at 25 °C. Afterwards, the CM-H_2DCFDA-loaded RBCs were washed once with PBS and incubated for a short recovery time of 10–15 min in order to render the dye responsive to oxidation. Fluorescent DCF production was measured using the VersaFluor™ Fluorometer System (Bio-Rad) at 490 nm excitation and 520 nm emission wavelengths. Intensity records were normalized to the protein level (~1.0–2.0 mg/ml). CM-H_2DCFDA sensitivity to ROS detection was verified in H_2O_2- or t-BHP-treated stored RBCs suspensions. The following negative controls were used: (1) unstained RBCs incubated with only PBS buffer to detect auto-fluorescence, and, (2) cell-free mixtures of dye and buffers.

For the intracellular calcium measurement, L- and N-RBCs were resuspended (final HCT 0.32–0.64%) in a buffer containing 145 mmol/L NaCl, 7.5 mmol/L KCl, 10 mmol/L Hepes/NaOH, 1.8 mmol/L $CaCl_2$, 10 mmol/L glucose and 10 mmol/L sodium pyruvate (pH 7.4). The cells were loaded with the membrane-permeable acetoxymethyl ester derivative of the fluorescent calcium indicator Fluo-4 (Fluo-4 AM) at 2 μmol/L final concentration for 40 min at 37 °C, in the dark [24]. Following wash in dye-free buffer, the cells were incubated for a further 30 min at room temperature. The fluorescence intensity of Fluo-4 AM after the binding of intracellular calcium was measured in the VersaFluor™ Fluorometer System at 485 nm excitation and 520 nm emission wavelengths. The possible degradation of the AM ester aliquots and the responsiveness of the dye to the RBCs cellular environment (use of A-23187 ionophore in a control experiment) were checked before each assay, according to the manufacturer's guidelines. Each sample was measured in triplicate.

2.6. Treatment of RBCs

In order to evaluate the tyrosine phosphorylation of band 3, we treated L- and N-RBCs with ortho-vanadate that is a protein tyrosine phosphatase inhibitor. Tyrosine phosphorylation state of a protein is the result of the competing activities of protein tyrosine kinases and protein tyrosine phosphatases. In human RBCs tyrosine phosphatases activity is very high in relation to that of tyrosine kinases, resulting in a low basal phosphotyrosine level. As a result, tyrosine phosphorylation of band 3, constituting the major site of phosphorylation, cannot be detected in untreated RBCs [25,26]. However, upon treatment with protein tyrosine phosphatases inhibitors a large increase in erythrocyte protein tyrosine phosphorylation is observed. Ortho-vanadate induces hyper-phosphorylation of band 3 on tyrosine residues probably by inhibition of RBCs tyrosine phosphatases. The mechanism underlying the activation of tyrosine phosphorylation is thought to involve the sequential action of two protein tyrosine kinases, Syk (p72syk) and Lyn (p53/56lyn) and probably some type of protein conformational change in the membrane skeleton that generate a new or more accessible binding site that is otherwise occluded or inaccessible in no stimulated cells [27]. To detect tyrosine phosphorylation, stored L- and N-RBCs were diluted (at 30% HCT) in PBS containing 5 mmol/L glucose (PBS-glucose) and incubated with 2.0–2.5 mmol/L ortho-vanadate for 2 h at 37 °C. For controls, RBCs were either left untreated or pretreated (before addition of o-vanadate) with 1 μM Syk inhibitors II and IV for 1 h at 37 °C in the dark. Each reaction was stopped by washing with PBS-glucose. For membrane preparation phosphatase inhibitors were included to the cell lysis buffer.

The ability of chemical cross-linkers to cross-link band 3 in stored RBCs was assessed by incubating RBCs (~25×10^6 cells/ml) with 1.0–2.5 mmol/L bis-sulfosuccinimidyl-suberate (BS3) in non-amine-containing conjugation buffer (20 mmol/L sodium phosphate, 150 mmol/L NaCl, pH 8.0) for 30 min at 20 °C. RBCs were then washed in quenching buffer (150 mmol/L NaCl, 25 mmol/L Tris pH 7.4), to inactivate residual cross-linking agent. After both treatments, membranes were prepared and analyzed as described below.

2.7. Density fractionation of RBCs

RBCs' fractionation according to density was performed by means of a Percoll discontinuous gradient as previously described [28,29]. Briefly, the gradient was built up in five layers of Percoll medium varied between 1.087 and 1.098 g/ml. RBCs suspensions (40% HCT) were layered on the top of the gradients and the fractions were collected by low speed centrifugation (2700 ×*g*) for 40 min at 20 °C. Cells were excessively washed to remove Percoll and a range of age-dependent RBCs parameters were recorded in each fraction (MCV, MCHC etc.).

2.8. Isolation of vesicles and RBCs-membrane preparation

Vesicles were isolated from the supernatant of L- and N-RBCs units (n=4) on days 17 and 42 of storage by high-speed centrifugation at 4 °C as previously described [30,31]. Briefly, RBCs aliquots were centrifuged at 2000 ×*g* and the supernatants filtered through sterile 0.8 μm nitrocellulose filters. The filtrate was ultracentrifuged at 37,000 ×*g* for 1 h and the pellet of vesicles was resuspended in PBS and ultracentrifuged twice under the same conditions. After the addition of protease inhibitors mix, the protein concentration was determined using the Bradford protein assay. Quantification of the extent of

vesiculation was based on the total protein content of the vesicle suspensions in relation to the volume of the RBCs as previously described [31]. To our knowledge, this method along with that of centrifugable Hb estimation, have an advantage over the less laborious and cell-specific flow cytometry approach in that they allow the analysis of smaller (less than 200–300 nm) microvesicles.

RBCs were isolated by the method of Beutler [32]. Briefly, leukocytes and platelets were removed from the RBCs samples by filtering through columns of alpha-cellulose and microcrystalline cellulose mixture in isotonic saline, PBS or Hepes-buffered isotonic saline (133 mmol/L NaCl, 4.5 mmol/L KCl and 10 mmol/L Hepes, pH 7.4) supplemented with protease inhibitors. RBCs were extensively washed and diluted to an appropriate HCT. Purified RBCs were lysed with hypotonic (5 mmol/L) sodium phosphate buffer (pH 8.0) containing a cocktail of protease inhibitors and membrane fractions were prepared as previously described [17].

2.9. Immunoblotting analysis and estimation of membrane proteome carbonylation index

Equal amount (12–25 μg) of RBCs total membrane protein was loaded in Laemmli gels, blotted to nitrocellulose membranes and probed with primary and HRP-conjugated secondary antibodies. Immunoblots were developed using an ECL reagent kit and quantified by scanning densitometry (Gel Analyzer v.1.0 image-processing program, Athens, Greece). Purified RBCs plasma membrane proteins were processed for the detection of carbonyl groups using the Oxyblot detection kit as per manufacturer's specifications. For quantification purposes, the proteome carbonylation index (PCI) was calculated [21].

2.10. Statistical analysis

Presented experiments have been repeated at least two times, unless otherwise stated. Data points correspond to the mean value; error bars denote SD. Individual protein levels were quantified against a reference membrane protein or against the sum of the normal proteins, occasionally further normalized to the respective corresponding controls (untreated, non-stored, L-RBCs, or young cells). For statistical analysis the MS Excel and the Statistical Package for Social Sciences (IBM SPSS; version 19.0 for Windows; administrated by NKUA) were used. Significance was evaluated using the one-way ANOVA. Comparisons between different groups were performed by the independent t-test or the chi-squared test. Spearman's correlation test (two-sided) was used to assess the relationship between variables (correlation coefficient r). Significance was accepted at $p<0.05$.

3. Results and discussion

3.1. Supernatant composition and hematological profile differences between L- and N-units

Storage resulted in increased hemolysis and potassium release in both groups throughout the entire storage period (Table 1). L-units were characterized by substantially higher hemolysis and supernatant potassium compared to the N-units ($p<0.05$) on the day of donation. However, afterwards and until the end of the storage period both parameters were significantly higher in N-RBCs ($p<0.05$) as expected [9,10]. Storage of both groups was also associated with a significant elevation of MCV after the first week as previously reported [33], equally processed for L- and N-RBCs until the last day. After prolonged storage the RDW index of N-RBCs was also substantially higher compared to the L-RBCs.

The increased hemolysis seen in L-units on the day of donation probably relates to donor variations regarding the leukoreduction procedure. Indeed, as previously observed [9], the RBCs from some healthy individuals are more susceptible to hemolysis during the filtering than other. On the other hand, the RDW index variation probably reflects the N-RBCs-related increase in spherocytosis and cellular fragmentation. Notably, in renal disease patients the aberrant RDW was found positive correlated to the degree of echinocytosis and intracellular ROS accumulation [21].

Table 1 – Hematological analysis and supernatant biochemical data for L-RBCs and N-RBCs units (n=8).

	Non-leucodepleted units (N)				Leucodepleted units (L)			
	Day 0	Day 20	Day 30	Day 42	Day 0	Day 20	Day 30	Day 42
WBCs ($\times10^3/\mu L$)	8.1±0.0*	7.7±0.0*	5.1±0.5*	4.4±1.0	0.3±0.0	nd[a]	nd[a]	nd[a]
RBCs ($\times10^6/\mu L$)	8.4±0.8	8.5±1.3	8.6±1.1	8.6±1.1	8.3±0.1	8.2±0.1	8.1±0.0	8.1±0.0
PLTs ($\times10^3/\mu L$)	283±10	203±2	179±81	151±71	nd[a]			
Hb (g/dL)	22.7±0.4	23.0±0.1	23.4±1.1	23.4±1.2	22.4±1.5	23.0±2.5	22.8±2.0	22.7±2.3
Hct (%)	80.0±11.5	80.0±11.2	83.3±9.8	83.2±10.0	75.6±1.8	76.7±0.6	77.5±2.0	77.0±1.6
MCV (fL)	90.0±2.4	94.8±1.6	97.1±1.0	98.2±1.0	88.9±2.5	93.1±2.1	95.6±2.7	96.5±3.0
MCH (pg)	30.8±2.0	31.5±1.0	31.5±0.6*	32.1±0.4	30.3±0.1	30.1±0.6	30.1±0.4	31.3±1.5
MCHC (g/dL)	31.3±0.3	31.7±0.4	31.8±0.1	32.3±0.3	30.8±0.8	31.5±1.3	31.1±1.0	32.0±0.4
RDW-CV (%)	12.7±0.7	14.6±0.2	15.8±0.8	16.7±0.6*	11.7±0.6	14.1±0.4	14.6±0.4	15.6±0.4
Supernatant Na^+ (mmol/L)	139.5±0.7*	84.0±1.4*	79.5±2.1	67.5±0.7	142.5±0.7	89.0±2.8	81.5±2.1	62.5±2.1*
Supernatant K^+ (mmol/L)	4.4±0.3	16.9±0.8*	24.3±3.6	35.8±1.5*	6.0±0.1*	15.1±0.3	21.0±0.4	26.3±0.6
Hemolysis (%)	0.13±0.06	0.59±0.21*	0.72±0.24*	1.48±0.33*	0.33±0.01*	0.24±0.05	0.30±0.02	0.70±0.11

Results are presented as mean±SD.
[a] Non-detected (less than detection limit).
* $p<0.05$ L-RBCs vs. N-RBCs.

3.2. *Effect of residual leukocytes on RBCs structural integrity and membrane preservation*

We analyzed the morphology of L- and N-RBCs by means of scanning electron microscopy at three time points of the storage period (n=8). We used the previously established criteria for the classification of the irreversibly shaped RBCs (all spherocytic cells and that of degenerated shapes, see index in Fig. 1A) but more strict criteria for the category of normal discocytes, by classifying as such only the perfectly shaped cells (see Materials and methods). RBC morphology was deteriorating with increasing storage time in both groups (Fig. 1A). However, while at the beginning of the storage the two groups exhibited an equal percentage of shape changes (Fig. 1B), on day 21 and afterwards there was a significant increase ($p<0.050$) in the irreversible transformations in N-RBCs compared to the L-RBCs. This finding is probably associated with the extent of vesiculation and membrane loss observed in N-RBCs after the second week of storage (see below). Towards the end of the storage period, the gap divergence in the percentage of irreversible transformations between the two units was narrowed (still however significant), probably in relation to the N-RBCs hemolysis (Table 1).

We next estimated the degree of vesiculation, expressed as the total protein of the collected vesicles per volume unit of RBCs (μg/ml). The vesiculation was increased in both groups (n=4) over storage time (Fig. 2), as previously reported [1,31]. Nevertheless, there was a statistically significant increase in the amount of vesicular protein collected from the N-RBC supernatants compared to the L-RBC ones on the 17th day, which was maximized at the end of the storage period ($p<0.010$, 3.3–27.7 μg/ml and 9.2–51.8 μg/ml for the L- and N-units, respectively).

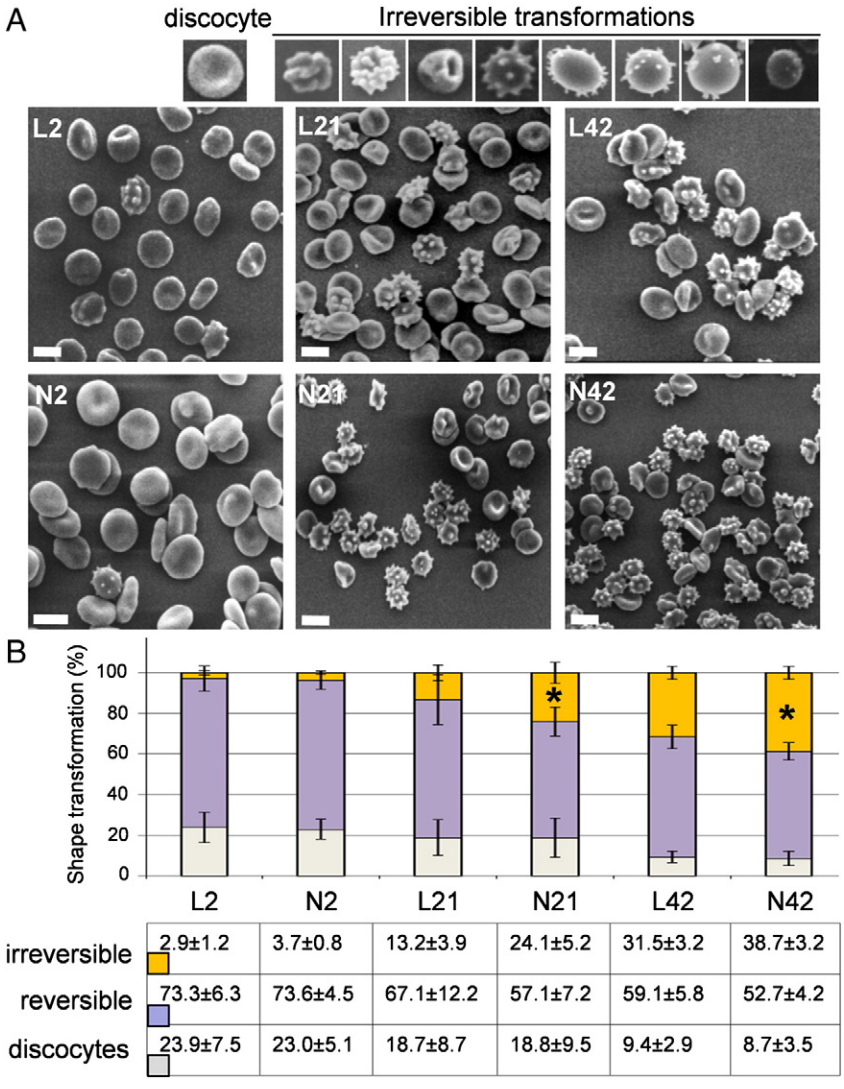

	L2	N2	L21	N21	L42	N42
irreversible	2.9±1.2	3.7±0.8	13.2±3.9	24.1±5.2	31.5±3.2	38.7±3.2
reversible	73.3±6.3	73.6±4.5	67.1±12.2	57.1±7.2	59.1±5.8	52.7±4.2
discocytes	23.9±7.5	23.0±5.1	18.7±8.7	18.8±9.5	9.4±2.9	8.7±3.5

Fig. 1 – Morphologic evaluation of L- and N-RBCs by scanning electron microscopy during the storage in CPD-SAGM. (A) Index of "irreversible" RBCs transformations and representative electron micrographs from a donor's RBCs stored in either L- or N-units for 2, 21 or 42 days. Scale bars, 10 μm. (B) Average percentage of discocytes, reversibly and irreversibly (see Materials and methods) changed stored RBCs for the indicated storage time-points. Error bars indicate SD (n=8); (*) L- vs. N-RBCs $p<0.01$ and <0.05 for the days 21 and 42, respectively.

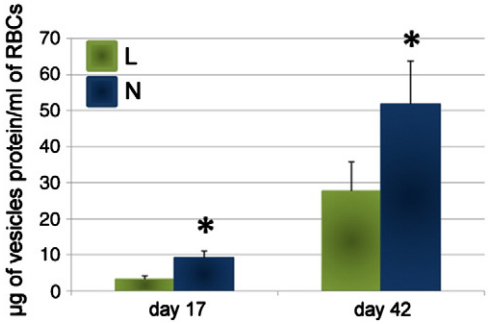

Fig. 2 – Vesiculation degree of L- and N-RBCs. Comparative estimation of the averaged total vesicular protein content per volume of packed RBCs, collected from the supernatant of both groups on days 17 and 42 of storage. Error bars indicate SD (n=4); (*) p<0.01 L- vs. N-RBCs.

During storage, RBCs undergo a progressive change in shape, from discocytes to echinocytes and finally to spherical and degenerative shaped cells, closely associated with membrane loss in the form of microvesicles [34]. Although the average stored cells appear to be able to compensate for a moderate membrane loss following the replacement of the echinocytogenic medium (reversibly modified cells), the final spheroechinocyte stage is an irreversible outcome [34]. Indeed, spheroechinocytes are dying or about to die cells, with very short life expectancy and post-transfusion viability [35]. Greenwalt et al., [36] has found improved RBCs morphology and microvesiculation in L-units compared to the non-leukoreduced ones using phase microscopy, while the opposite finding was recently reported at confocal laser scanning microscopy level [15].

The membrane vesiculation results evidenced the clinically significant accumulation of more microvesicles inside the N-RBCs units compared to the L-ones. Undoubtedly, in the case of L-units those vesicles are released almost exclusively from the stored RBCs, representing a direct measure of the membrane surface loss. In the case of N-units however, the precipitable material inevitably contains vesicles released from the contaminant leukocytes and platelets as well. Although the cellular origin of the vesicles collected from the N-units is outside the scope of our study, it is expected that the great majority of them was produced by RBCs membrane vesiculation. In view of (i) the high ratio of RBCs to leukocytes and platelets (1 leukocyte per 2000 RBCs at the end of the storage period, see Table 1), (ii) previous studies showing that the majority of the vesicles collected from N-units of packed RBCs contain Hb [31] and (iii) the significantly increased echinocytosis of N-RBCs compared to the L-RBCs (Fig. 1), it is unlikely that the two- or three-fold increase in vesicular protein detected in N-units compared to the L-units is attributed to the vesiculation of the contaminant cells. Instead of that, it probably reflects the detrimental effect of residual leukocytes and platelets on N-RBCs membrane preservation.

Microvesiculation of the membrane contributes to the elimination of oxidized, damaged and signaling effective components from RBCs [37]. At the same time, vesiculation and irreversible transformation is part of the RBCs aging phenotype, both *in vitro* and *in vivo* [38]. The shape modifications of stored cells are associated with rheologic changes, increased viscosity and reduced flow in capillary systems [34]. Degenerative shape modifications and loss of membrane surface contribute to deformability defects that threaten post-transfusion viability of stored RBCs [6,22]. They also result in the release of vesicles that are rich in oxidized material, death signaling mediators and PS. The specific composition of the vesicles renders them highly pro-inflammatory and pro-thrombotic, increasing thus the risk of adverse post-transfusion reactions. As a result, the degree of vesiculation and irreversible transformation of stored RBCs have been used as measures of storage quality [39]. Despite that, the identity of the storage parameters that slow or promote vesiculation, is still elusive. *In vitro*, both echinocytosis and microvesiculation are promoted by intracellular calcium elevation and ATP depletion but during routine storage this correlation is poor [40]. According to our results (see below) the poor preservation of proteins that contribute to the effective adhesion of cytoskeleton to the lipid bilayer, seems a plausible alternative explanation. In support, the effect of cytoskeleton protein damage to the vesiculation susceptibility of stored cells has been previously reported [41]. In conclusion, the comparative analysis of L- and N-groups showed that the residual leukocytes and platelets militate against the structural integrity and membrane preservation of stored RBCs.

3.3. *The contaminant cells exacerbate PS exposure on N-RBCs*

Annexin V binding by RBCs was assessed over storage time by means of fluorescent microscopy. In view of the very low presentation of other cell types in the samples (Table 1) and their effective discrimination by size and morphology criteria, only the RBCs of the units were included in the measurements. Our approach revealed a small but significant and progressive increase in PS externalization of both groups' RBCs (n=8) during the storage (Fig. 3). In agreement with previous studies documenting PS exposure on RBCs already after the first day of storage [42], we detected a significant increase (p=0.028) in PS-positive cells on day 5 (L 2.56±0.38% and N 3.75±0.67%) compared to the scanty percentage observed in the non-stored blood of the same donors (L 0.09±0.01% and N 0.11±0.01%). Likewise, the N-units contained on average more PS-positive RBCs compared to the L-units in the middle of the storage period (4.69±0.50% vs. 3.45±0.29%, p=0.019), however near the last days the differences were flattened following a trend for greater PS exposure in L-RBCs (6.90±0.70% vs. 6.13±0.63% in N-RBCS). Probably, the higher vesiculation (Fig. 2) and hemolysis (Table 1) levels result in a smaller subpopulation of PS-positive aged RBCs in N-units [43,44]. On the last day of storage an obvious difference between the two groups appeared at the fluorescence microscopy level, where the N-RBCs of all donors examined were surrounded by a dense "cloud" of PS-positive particles of 1 µm or less in size (arrows in Fig. 3, photo N42) which probably represent RBCs-derived microvesicles [34].

Since PS externalization is a potent removal signal, it might menace *in vivo* viability of stored RBCs [45]. In overall, PS exposure in both L- and N-RBCs is rather low, reflecting the previously

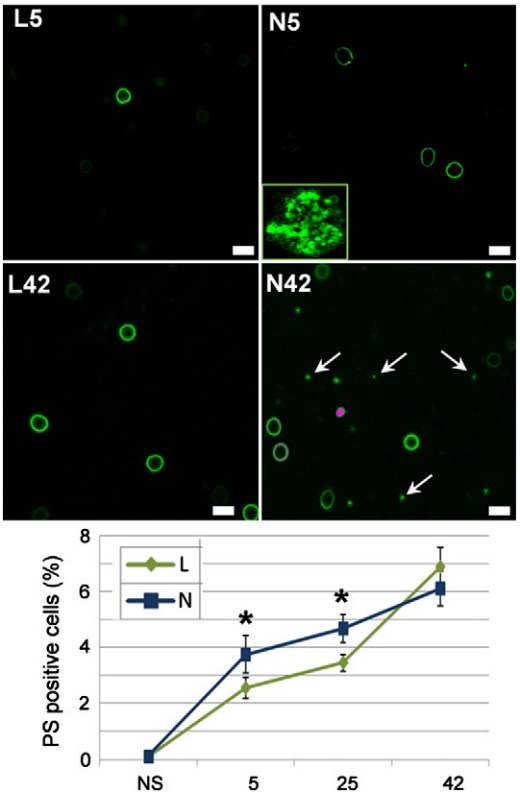

Fig. 3 – PS exposure on stored RBCs. L- and N-RBCs were stored for various days in CPD-SAGM and their PS exposure was determined by CLSM using fluorescently labeled annexin V. Representative CLSM images from a donor and the average percentage of PS-positive RBCs in both groups during the storage are shown. Scale bars, 10 μm. Insert in image N5: apoptotic leukocyte. Arrows in image N42: Small (less than 1 μm) PS-positive particles seen after prolonged storage. NS: non-stored RBCs of the same donors. Error bars indicate SD (n=8); (*) p<0.05 L- vs. N-RBCs.

documented intrinsic capability of stored RBCs in preserving membrane phospholipid asymmetry [46]. This finding has been associated with the very low levels of scrambling activity during storage in spite of a reversible decrease in ATP, pH and flippase activity levels [46,47]. Although there is no clear consensus whether a fraction of stored erythrocytes expose PS [48,49], according to our results the prolonged storage seems to overcome the physiological competence of the cells, even of the leukoreduced ones, confirming earlier data [44,46]. Residual leukocytes and platelets are definitely not the cause of increased PS exposure, but they seem to exacerbate it in both RBCs and supernatants, as previously reported by others [49–51]. Several mechanisms have been proposed to interpret this effect, like the increase in intracellular calcium and the release of leukocyte-derived neuraminidases [50]. The transfer of PS to RBCs by fusion of vesicles shed by contaminant cells undergoing apoptosis, vesiculation and lysis [52,53] during refrigerated storage (see insert in Fig. 3 photo N5) cannot be excluded. This finding is of clinical importance in light of studies showing that PS expressing N-RBCs exerts procoagulant effects [43] and increased adherence to the endothelium [54].

3.4. *Differences in the calcium and ROS accumulation between L- and N-RBCs*

We next asked whether RBCs storage in the presence or absence of contaminant cells would have any effect in the intracellular calcium levels. For that purpose, stored L- or N-RBCs (n=8), without any stimulation *in vitro*, were loaded with the fluorescent calcium reporter Fluo-4 and the fluorescence intensity was measured by fluorometry. Although there is a probable effect of SAGM-induced MCV modifications to the Ca^{2+} measurement performed, this is expected to affect equally the two groups (L and N) of SAGM-stored RBCs. Our results (Fig. 4) show that intracellular calcium increased slowly, but gradually on day 7 onwards in both groups ($p<0.05$, NS vs. day 7), with the N-RBCs exhibiting constantly higher levels of calcium compared to the L-RBCs in all donors and time-points (n=8) examined. The fluorescence intensity was peaked on day 38, followed by a drop on the last day of storage in both groups (Fig. 4). Although the only significant difference in calcium accumulation between the L- and N-RBCs was detected on day 29 of storage ($p<0.01$), the total storage-induced calcium accumulation in N-RBCs was higher compared to that of L-RBCs in paired comparisons ($p<0.05$).

There is evidence that free calcium content of human RBCs is a parameter of cell aging *in vivo* and *in vitro* [2,55]. The increase in intracellular calcium, accompanying either RBCs senescence or *in vitro* imposed stressful stimuli, directly induces or indirectly promotes a cascade of molecular and cellular events like potassium leakage, cellular dehydration and shrinkage, loss of deformability, echinocytosis, protein degradation/crosslinking,

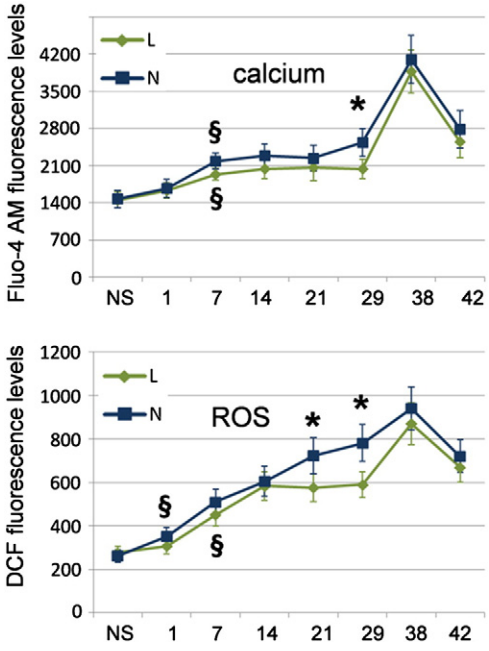

Fig. 4 – Graphs showing the averaged intracellular calcium and ROS accumulation in L- and N-RBCs throughout the storage. Data represents the mean ± SD (error bars, n=8) of Fluo-4AM (for calcium) or DCF (for ROS) fluorescence levels estimated by independent experiments done in triplicates. NS: non-stored RBCs of the same donors. (*) p<0.05 L- vs. N-RBCs. (§):p<0.05 vs. NS RBCs.

recognition signaling and eryptosis [2,56,57]. Calcium accumulation has been characterized as a probable secondary mediator of injury in stored RBCs in the past [58]. Indirect manifest of calcium activity in stored RBCs came by the finding that the storage-dependent remodeling of the RBCs membrane includes the calcium-promoted binding of sorcin and synexin [3]. However, other studies reported that there is not significant rise in intracellular calcium levels during storage, especially in L-RBCs [40,59].

Our results suggest that the residual leukocytes and platelets aggravate to an extent the calcium accumulation in stored RBCs. In addition, according to our measurements, short storage in CPD-SAGM stimulates a little calcium increase in stored RBCs but after the 4th or 5th week for the N- and L-units respectively, the storage effect is more stressful, irrespectively of the leukoreduction. This storage-related profile of calcium variation is especially interesting in light of reports showing the dual action of calcium-activated calpain on the calcium pump. At low calcium levels and short exposure times, calpain markedly increases ATP hydrolysis and pump activity while at high calcium concentrations or long exposure times, calpain action results in a progressive pump degradation, loss of pumping activity and membrane protein degradation [60]. Since our study did not involve an absolute measurement of intracellular calcium concentration, the question of whether the distortions observed have the potential to trigger calcium signaling activity, cannot be answered in direct. Despite that, in combination with the structural, PS and vesiculation data they pointed out a differentiation in the RBCs aging phenotype that might be partially associated with the calcium homeostasis under conditions implicated or no pre-storage leukoreduction.

In order to estimate the ROS accumulation in stored L- and N-RBCs ($n=8$), we used the redox-sensitive dye CM-H_2DCFDA. Compared to the non-stored cells of the donors (Fig. 4), in N-RBCs there was a gradual increase in ROS levels already from day 1 onwards ($p<0.05$, NS vs. day1). In L-units increase in ROS levels begun later on, after the first week ($p<0.01$, NS or day 1 vs. day 7), in line with previous data showing that 7 days of storage of L-RBCs double the levels of baseline ROS [61]. Moreover, unlike N-RBCs, ROS accumulation in L-RBCs reached a plateau in significantly lower levels than N-RBCs ($p<0.05$) during the middle of the storage period (Fig. 4). This finding was consistent with the recently reported study of Zolla's group in L-RBCs [23]. The fluorescence intensity was peaked on day 38 and significantly reduced on the last day of storage in both groups (Fig. 4), similarly to both intracellular calcium levels and membrane PCI fluctuation (see below). The reduction in ROS levels shown on the last days of storage might be attributed to the leakage of the probe from the leaky, hemolyzed RBCs, to the lower concentration of Hb and to the lower activity of cellular esterases in senescent RBCs, as previously reported [61,62]. As a result, statistically significant difference in ROS levels between the L- and N-RBCs was observed from the 3rd to the 4th week of storage ($p<0.05$). In summary, our analysis revealed that ROS accumulation is a very early manifestation in stored RBCs in the presence of contaminant cells while pre-storage leukoreduction can alleviate the impact of storage on cellular oxidative stress. Furthermore, our study defines the fifth week of storage in CPD-SAGM as a critical period regarding the levels of intracellular ROS.

Intracellular oxidative injury has been demonstrated during both RBCs *in vivo* and *ex vivo* aging [1,2,4,17]. According to our results the duration of storage accentuate the intracellular ROS accumulation in greater extent than the calcium accumulation in both groups (Fig. 4). ROS origin could be ascribed to cell senescence, Hb oxidation, decomposition of membrane lipids and finally, to metabolism-associated changes in cellular antioxidant defenses [1,63–65], that contribute to reduced post-transfusion survival [66]. Leukocytes are thought to accelerate the rate of storage lesion by at least two ways: before their breakdown, they consume glucose supplies and create waste products while after their breakdown they release enzymes, toxic and biologically active compounds that can hurt RBCs [10]. Indeed, leukocyte-derived free radicals are capable of evoking oxidative damage and hemolysis to stored RBCs [11,67], while significantly higher glucose consumption has been reported in N-units [68]. In our samples, pre-storage leukocyte/platelets removal reduced the levels of intracellular ROS only before the 4th week of storage, but afterwards both groups showed similar levels of ROS (Fig. 4), suggesting that mechanisms independent of the contaminant cells effect contribute to RBCs oxidative stress in the later period of storage. These findings support previous reports showing that oxidative burst/potential of neutrophils by stored RBCs supernatants was not significantly reduced by leukoreduction [69]. Whatever the possible sources of intracellular ROS might be, the leukoreduction is expected to be connected to lower oxidative stress in stored RBCs, which according to the literature, might be reflected in aging and death signaling, membrane deformability and vesiculation [41] as well as in lipid/protein oxidative damage profiles [11].

3.5. *Membrane proteome remodeling in L- and N-RBCs*

Significant increase in tyrosine phosphorylation of band 3 was observed between the 4th and 5th week of storage in both units (Fig. 5A), at the same time when the peak in intracellular ROS and calcium levels was evident (Fig. 4). Band 3 tyrosine phosphorylation predominated in N-RBCs compared to the L-RBCs on day 28 measurements ($n=8$), while towards the end of the storage period the two groups contained practically equal levels of phosphorylated band 3 (Fig. 5A). This happened in striking timing correlation with the observed kinetics of ROS and calcium measurements (compare Figs. 4 and 5A). Since only the oxidized fraction of band 3 is phosphorylated – and thus dissociated from the underlying cytoskeleton – under the trigger of oxidative stress [70], the higher levels of phosphorylated band 3 in N-RBCs might also be associated with the greater vesiculation of the same group vs. L-group (Fig. 2), as previously observed in ortho-vanadate-treated non-stored RBCs [26]. By the same way, the compensated levels of tyrosine phosphorylation between the two groups after the 5th week of storage (Fig. 5A) could reflect the average effect of increased oxidative stress and vesiculation in N-RBCs.

To estimate the cross-linking potential of band 3 in L- and N-RBCs stored for 4 weeks in CPD-SAGM, we treated RBCs suspensions with BS3, a membrane impermeable cross-linking agent known to cross-link band 3, and examined the relative percentage of the resulting high molecular weight band 3 aggregates. According to our results (Fig. 5B), the N-RBCs were more susceptible to the BS3-induced cross-linking of band 3

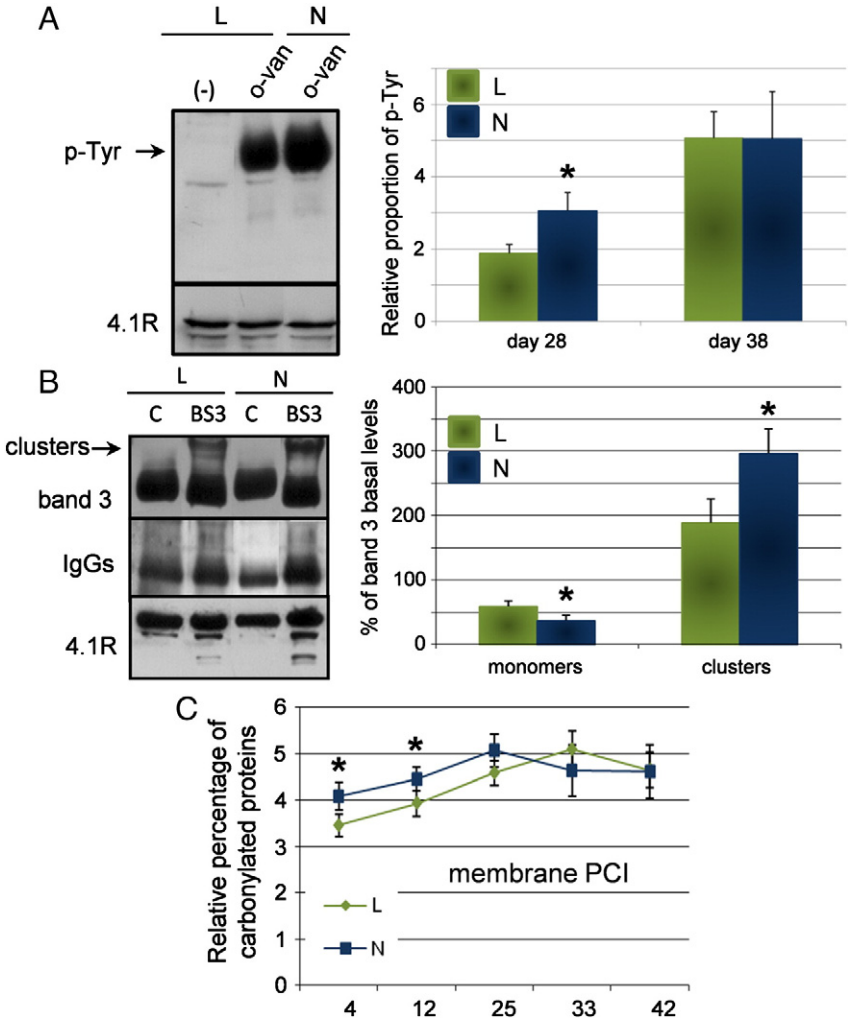

Fig. 5 – Band 3-associated signaling modifications and membrane proteome carbonylation index (PCI) in stored RBCs. (A) Tyrosine phosphorylation (p-Tyr) of band 3 in ortho-vanadate-treated (o-van) L- and N-RBCs stored for 28 or 38 days. Representative immunoblot analysis [(–): control, see Materials and methods] and bar graph representing the averaged (n=8) relative proportion of p-Tyr band 3 (normalization to the endogenous 4.1R protein levels) in L- and N-RBCs, are shown. (B) Cross-linking potential of band 3 and IgGs binding in BS3-treated RBCs stored for 4 weeks in CPD-SAGM. Representative immunoblots and bar graph representing the mean (n=8) percentage of band 3 clusters as well as of monomeric band 3 left in BS3-treated cells (normalization to the basal band 3 levels), are shown. (C) Graph showing the collective densitometric analysis of membrane PCI levels variation in stored RBCs in relation to the leukoreduction. Error bars: SD; (*): $p<0.05$ L- vs. N-RBCs.

compared to the L-RBCs. That finding was established by measuring both the relative percentage of band 3 clusters (297%±38% vs. 188±37%, respectively, $p<0.05$) as well as the concomitant depletion of monomeric band 3 (37±8% vs. 59±8%, respectively), after normalization to the basal levels (untreated RBCs, n=8). Moreover, as shown in Fig. 5B (left panel), there was increased membrane binding of IgGs in the N-RBCs compared to the L-RBCs, roughly analogous to the levels of band 3 oligomerization.

Band 3 possesses a core position in RBCs senescence and death signaling mechanisms. Structural and functional modifications of this protein, like proteolysis, clustering and increased tyrosine phosphorylation, are major senescence-associated changes in the currently established models [2,71]. Apart from senescence, tyrosine phosphorylation of band 3 is induced by various stimuli including oxidative and calcium stress [1,25,70,72] and it enhances the lateral mobility of the protein and its cross-linkability [26,70]. All these band 3-associated modifications are correlated with significant changes in RBCs morphology and vesiculation through changes in the membrane-cytoskeletal interactions [26]. Our findings are totally consistent with previous reports showing that naturally occurring IgGs binding to the RBCs surface depends on the band 3 oxidation/oligomerization state [73] and that the band 3 tyrosine phosphorylation-induced clustering is associated with IgGs binding [70].

We next estimated the membrane proteome carbonylation index (PCI) of the L- and N-RBCs by means of immunoblotting. As expected, prolonged storage aggravated the membrane protein carbonylation in both groups (n=8, Fig. 5C). The PCI increased constantly from day 4 to day 25 (N-RBCs) or day 33 (L-RBCs) where the peak of ROS levels was also observed, while afterwards there was a trend for stabilization to lower levels, as

previously reported [17,23,74]. By the same manner, the N-RBCs were characterized by higher values of PCI compared to the L-RBCs until the middle of the storage period ($p<0.05$), but afterwards there was no significant differences between the two groups (Fig. 5C).

The PCI has been widely used as a measure of membrane and plasma protein injury in storage, where it has been found distorted, in correlation to both the storage length (days) [74] as well as the preservation medium [17]. In our study, the pattern of PCI variation seen after prolong storage in L- and N-RBCs (plateau formation and balancing between the groups, Fig. 5C) might be associated with the extent of vesiculation that leads to the clearance of the carbonylated material [31], the hemolysis of the severely damaged RBCs [17] as well as with storage-related changes in the membrane binding of enzymatic, proteolytic and chaperone components [75].

Further on, we tested our samples for another potential oxidative stress biomarker [76], the membrane-bound Prx2. We detected gradually increased membrane association of Prx2, under both reducing (Fig. 6A) and non-reducing (Fig. 6B) conditions in L- and N-RBCs (n=8). Although there was an obvious donor variability regarding the Prx2 membrane levels (reflected in the high SD values), probably associated with the RBCs antioxidant capacity of each donor [76], the monomeric and dimeric forms of membrane Prx2 exhibited not only positive correlation to the duration of storage (correlation coefficient $r=0.852$) but also significant ($p<0.05$) increase in the case of N-RBCs compared to the L-RBCs (Fig. 6B). In some cases, the N-RBCs were characterized by a transient increase in Prx2 levels on the first days of storage that was afterwards normalized to the anticipated storage variation pattern (see right panel in Fig. 6A). Membrane-bound Prx2 was further proportional to the expression of a wide array of senescence and oxidative stress markers on RBCs membrane, including autologous IgGs binding and cross-linkings of Hb (see below Fig. 6C and Table 2), as previously shown in both storage and hereditary spherocytosis [17,77].

The highly abundant erythrocytic Prx2 is a 2-cys peroxiredoxin that functions as an antioxidant enzyme in the disposal of endogenous H_2O_2 and also as a chaperone [78,79]. Its recruitment to the membrane has been described in the presence of increased intracellular calcium levels [80] as well as under various oxidative stress conditions [21,77], including prolonged storage [17,23,75]. According to previous reports, protein oxidation is the main contributor to the storage lesion seen in SAGM-stored N-RBCs [81]. The oxidative stress-associated progressive linkage of cytosolic proteins to the membrane has been repeatedly reported in RBCs stored under various conditions and mediums.

Table 2 presents the averaged variation (n=8) in the expression profile and Fig. 6C some representative cases of membrane protein variations observed during the storage of L- and N-RBCs. The overall membrane remodeling in both groups is a panel of protein modifications that have long been described in stored cells: significant loss of proteins and surface receptors (Table 2: spectrin, band 3, 4.1R, pallidin, CD47, protectin etc.), cytoskeleton proteins (spectrin and 4.1R) fragmentation, inter-protein conjugation (e.g. spectrin-Hb cross-linking) and recruitment of cytosolic proteins (oxidized/denatured Hb oligomers, HSP70) and plasma IgGs. Some of them are currently assessed as molecular

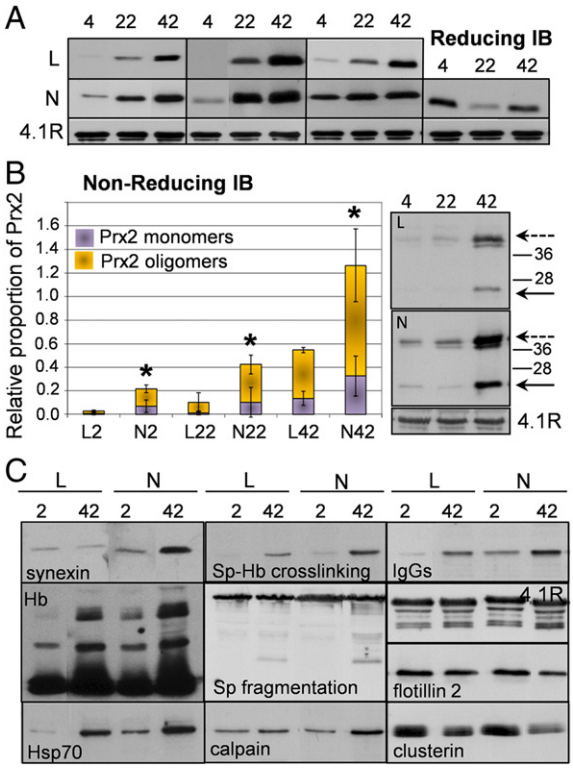

Fig. 6 – Membrane proteome remodeling during the storage of L- and N-RBCs. (A) Representative comparative immunoblot (IB) analysis under reducing conditions, for the presentation of donor variability in the membrane-bound Prx2. Four different donors are shown. (B) The same Prx2 analysis under non-reducing conditions, for the detection and quantitative analysis of membrane-bound Prx2 monomers and oligomers (indicated by solid and discontinuous arrows, respectively in Prx2 IB). Error bars: SD (n=8); (*) $p<0.05$ L- vs. N-RBCs. (C) Representative cases of membrane protein variations observed in L- and N-RBCs by immunoblot analysis. Membrane preparations of only day 2 and 42 are compared.

markers of senescence, vesiculation and cellular stress, including oxidative stress that may lead to the increased clearance of transfused cells [2,29,82].

In a comparative aspect, the presence of residual leukocytes and platelets in the labile product seemed to inflict extra proteome stress in the membrane, as documented by the significant diversification in the protein expression between the two groups examined (shown by asterisks in the Table 2). Indeed, common senescence biomarkers like the cross-linkage of spectrin with hemoglobin [83], the binding of oxidized/denatured Hb and IgGs as well as the loss of major sialoglycoproteins, exhibited higher expression in N-RBCs compared to the L-RBCs (Table 2, Fig. 6C). Towards the end of the storage period there was a greater deficiency in the CD47 protein, an erythrocyte marker of self, in N-RBCs (Table 2). Previous studies have reported that without prior leukodepletion, the stored units exhibit an increased population of senescent RBCs and increased *in vitro* phagocytosis [50]. Our findings hold with those conclusions and further suggest a probable correlation of the senescence phenotype with the intracellular ROS levels and the degree of

Table 2 – Membrane protein analysis in L-RBCs and N-RBCs during storage in CPD-SAGM.

	Days of storage					
Protein	4	12	19	25	33	42
Spectrin	**1.00±0.05**	**1.01±0.06**	**0.97±0.09**	**0.92±0.05** [b]	**0.83±0.06**	**0.80±0.04** [a]
	1.00±0.09	0.98±0.11	0.93±0.12	0.85±0.10 [b]	0.74±0.05	0.69±0.05
Band 3	**1.00±0.03**	**0.97±0.11**	**0.94±0.05** [b]	**0.87±0.04** [a]	**0.76±0.05**	**0.77±0.04** [a]
	1.00±0.04	0.99±0.06	0.90±0.07 [b]	0.76±0.05	0.71±0.06	0.66±0.06
4.1R	**1.00±0.03**	**0.94±0.04** [b]	**0.90±0.03**	**0.85±0.04**	**0.87±0.05** [a]	**0.82±0.08** [a]
	0.99±0.04	0.87±0.06 [b]	0.83±0.04	0.79±0.07	0.75±0.05	0.66±0.06
Pallidin (protein 4.2)	**1.00±0.06**	**0.95±0.08**	**0.98±0.07**	**0.85±0.06** [b]	**0.80±0.07**	**0.76±0.08**
	1.00±0.05	1.13±0.08	0.95±0.05	0.86±0.07 [b]	0.77±0.06	0.72±0.09
Major glycophorins	**1.00±0.08**	**1.09±0.05**	**0.96±0.07**	**0.88±0.07** [b]	**0.81±0.06**	**0.83±0.08** [a]
	1.00±0.05	1.05±0.06	0.99±0.05	0.88±0.05 [b]	0.72±0.07	0.62±0.07
Stomatin	**1.00±0.03**	**1.10±0.04**	**0.95±0.08**	**0.88±0.04** [b a]	**0.89±0.08** [a]	**0.86±0.07**
	1.00±0.05	0.97±0.05	1.00±0.09	0.73±0.06 [b]	0.63±0.09	0.76±0.05
Flotillin2	**1.00±0.03**	**0.98±0.05**	**1.01±0.07** [a]	**0.95±0.05** [a]	**0.83±0.06** [b]	**0.65±0.08**
	1.01±0.06	0.87±0.06 [b]	0.83±0.05	0.79±0.06	0.75±0.07	0.72±0.07
Protectin (CD59)	**1.00±0.06**	**1.18±0.12** [a]	**0.99±0.09**	**0.89±0.08**	**0.92±0.09**	**0.82±0.06** [b]
	0.87±0.07	0.91±0.12	0.85±0.08	0.80±0.11	0.85±0.09	0.75±0.08 [b]
CD47	**1.00±0.06**	**0.95±0.05**	**0.92±0.06**	**0.81±0.05** [b]	**0.86±0.04** [a]	**0.79±0.06**
	1.00±0.04	0.98±0.06	0.85±0.07 [b]	0.77±0.07	0.72±0.07	0.69±0.05
IgGs	**1.00±0.09**	**0.91±0.09** [a]	**1.60±0.17** [a b]	**2.48±0.36** [a]	**3.12±0.28** [a]	**2.63±0.34** [a]
	1.05±0.11	1.20±0.13	2.07±0.32 [b]	4.67±0.62	3.86±0.43	3.40±0.41
Spectrin, 4.1R	**1.00±0.12** [a]	**0.95±0.19** [a]	**1.23±0.19** [b a]	**1.32±0.21** [a]	**1.85±0.32** [a]	**1.55±0.32** [a]
Fragmentation	1.60±0.28	1.89±0.39	2.00±0.43	2.25±0.46	3.16±0.53 [b]	2.69±0.59
Spectrin-Hb	**1.00±0.13**	**1.49±0.27** [b a]	**2.73±0.42** [a]	**2.29±0.53** [a]	**2.55±0.41** [a]	**4.94±0.89** [a]
Cross-linking	1.00±0.15	4.11±0.94 [b]	4.85±1.10	5.86±1.34	7.61±1.42	12.24±2.12
Hb monomers	**1.00±0.07**	**1.21±0.22**	**1.12±0.19**	**1.32±0.19** [b]	**1.15±0.17**	**1.59±0.22**
	1.00±0.09	1.03±0.18	0.87±0.12	1.03±0.16	0.94±0.15	1.30±0.18 [b]
Hb oligomers	**1.00±0.18** [a]	**1.81±0.36** [b a]	**1.57±0.37** [a]	**2.57±0.56** [a]	**3.08±0.56** [a]	**5.62±1.26** [a]
	1.94±0.38	2.97±0.61 [b]	3.61±0.77	5.22±1.24	7.35±1.62	9.44±1.79
Calpain	**1.00±0.15** [a]	**1.06±0.19** [a]	**1.73±0.31** [b a]	**1.45±0.24** [a]	**2.31±0.47** [a]	**2.64±0.43** [a]
	1.38±0.17	2.22±0.38 [b]	3.96±0.73	2.63±0.45	4.31±0.79	4.65±0.83
Hsp70	**1.00±0.18** [a]	**1.06±0.23**	**1.36±0.23**	**1.96±0.32** [b a]	**2.52±0.34**	**3.08±0.58** [a]
	1.54±0.28	1.62±0.34	1.92±0.37	2.38±0.36 [b]	3.13±0.43	5.20±1.13
Clusterin	**1.00±0.08**	**1.07±0.10**	**0.93±0.08**	**0.85±0.06** [b a]	**0.87±0.06**	**0.78±0.08** [a]
	1.00±0.10	0.94±0.08	0.85±0.11	0.68±0.08 [b]	0.72±0.09	0.58±0.09

Bold characters: L-RBCs.
Results are presented as mean±SD after normalization to the day 4 values of L-RBCs (n=8).
[a] $p<0.05$ L-RBCs vs. N-RBCs.
[b] $p<0.05$ vs. day 4 of L- or N-group.

echinocytosis in stored RBCs, as previously reported in *in vitro* studies [84].

Spectrin and 4.1R proteolysis is increased after the 2nd week of storage to day 33 in L-RBCs (Table 2), in line with recent reports [23], while in N-RBCs it is detected earlier (Table 2). Notably, in both groups the cytoskeleton proteins fragmentation maximized on day 35 (Table 2), concomitantly with the peaking in the intracellular ROS and calcium levels (Fig. 4), substantiating a causative effect, as previously suggested [81]. Whatever its origin might be, proteolysis of cytoskeletal components is a triggering factor for membrane vesiculation by weakening the cohesion of the skeleton to the lipid bilayer, as further supported by the significantly increased number of echinocytes in N-RBCs.

Another prominent difference between the two groups examined, was the increased membrane binding of synexin (Fig. 6C) and calpain (Fig. 6C and Table 2) in N-RBCs. This is probably correlated to the variation in intracellular calcium levels, since the migration of both proteins to the membrane is a calcium-dependent procedure [85,86]. Increased calcium levels might up-regulate a number of enzymes (e.g. calpains) and processes (e.g. proteolysis) that lead to cellular dehydratation and protein degradation. Membrane-bound calpain in calcium-stressed RBCs challenges cytoskeleton fragmentation, while under the influence of activated transglutaminase 2, cytoskeletal proteins crosslinkings are observed [1]. Both actions obviously affect cytoskeleton plasticity and cellular deformability. The higher levels of calcium stress-associated modifications in the membrane proteome of N-RBCs might correspond to the higher degree of spheroechinocytosis and the significant loss of cellular deformability [34] compared to the minimally affected L-RBCs [33].

The comparative higher loss of vesicle-associated components [31,37,75,87], like band 3, stomatin, flotillin-2, clusterin, CD59 and CD47 (Table 2 and Fig. 6C) might be associated with the intent vesiculation of the RBCs membrane in the non-leukoreduced units. Previous studies have reported significantly higher CD47 loss from the stored RBCs membrane in the presence of leukocytes [49] that is largely due to the release of

the protein in the supernatant [88]. The significantly decreased expression of CD59 (protectin) in N-RBCs reported here is consistent with the loss of glycosylphosphatidyl-inositol (GPI)-linked glycoproteins during the storage, especially in the presence of leukocytes [89]. Since CD59 is a complement regulatory protein that functions to protect blood cells from autologous complement attack (assembly of membrane attack complex), it may potentially play a role in the *in vivo* survival of transfused RBCs. In addition, considering that the N-RBCs accumulate more senescent defects, the observed protein loss might also be associated with the triggered activity of RBCs proteasomes in order to effectively remove the non-functional components [90]. In support, the more prominent stress-responding [17,21,23] migration of the cytosolic chaperones HSP70 (Table 2 and Fig. 6C) and Prx2 (Fig. 6A, B) to the membrane of N-RBCs suggests that the storage in the presence of contaminant cells triggers the generation of modified proteins that need assistance by the repairing molecular machinery of the cell. Whether or not and to what extent this cellular defense mechanism is effective in protecting and stabilizing the damaged components, is apparently a function of the membrane vesiculation degree, since both proteins are sorted for vesiculation in stored RBCs [17,75].

3.6. *The residual leukocytes and platelets promote a premature senescence phenotype expression in N-RBCs compared to their age-mate L-RBCs*

Fractions enriched in RBCs of various ages can be obtained by Percoll gradient fractionation based on cellular density [91]. Therefore, we separated fractions enriched in young (low density, Y-RBCs) and senescent (high density, S-RBCs) RBCs of various storage periods from both groups (n=4) according to cell density and we compared the intracellular ROS and calcium accumulation, as well as the membrane PCI between cells of comparable density. Furthermore, the variation in a series of cellular aging and stress protein markers has been evaluated in the low-density RBCs fractions collected at three time points of storage.

In RBCs of all storage periods, increased cell density was associated with a decreased MCV ($p<0.01$) and a proportionally increased MCHC ($p<0.01$) (Table 3). To further validate the fractionation, the derived lower and higher density subpopulations were examined for the presence of well-established RBCs membrane proteome aging markers, such as cross-linking between spectrin and Hb [83], binding of oxidized/denatured Hb and structural modifications (proteolysis/clusterization) of band 3 [38,57,71]. Indeed, compared to the low-density cells, the densest RBCs fractions exhibited significantly increased ($p<0.05$) expression of all those markers (Table 3), verifying the predominance of senescent cells.

Almost all the high-density preparations examined (n=4) were characterized by an average increase in ROS and calcium intracellular accumulation as well as in the membrane PCI compared to the low-density ones (Fig. 7A–C). Calcium and oxidative damage accumulation, PS externalization and loss of deformability have been previously reported in senescent RBCs [44,55,57,92,93]. Notably, data have shown that upon calcium-loading the Y-RBCs restore their cell volume and deformability, while the S-RBCs become dehydrated and less deformable [93]. With the exception of calcium levels that were maximized in S-RBCs on day 36 of storage (Fig. 7B), both ROS levels (Fig. 7A) and PCI (Fig. 7C) were either stable or decreased compared to the day 23. This is probably related to the senescence and death progression, as reflected by changes in the membrane vesiculation, Hb concentration and esterase activity in S-RBCs [62,63]. No significant difference was observed in the ROS/calcium levels of S-RBCs between the L- and N-groups (Fig. 7A, B), except for the ROS levels on day 8 ($p<0.05$ L- vs. N-RBCs). Although not important, higher ROS accumulation was measured in the leukoreduced S-RBCs during the middle of the storage period in almost all the donors examined (n=4). On the opposite, significant higher membrane PCI was found in non-leukoreduced S-RBCs on days 23 and 36 of storage, vs. L-ones (Fig. 7C). This ratio was totally reversed towards the end of the period, probably as a result of the comparatively higher vesiculation and hemolysis seen in N-RBCs (Fig. 2, Table 1).

The comparative monitoring of the above mentioned storage-associated variations in the every time "younger" L- and N-RBCs of lower density outlines the storage lesion course in relation to the aging and cellular stress phenotype. As shown in

Table 3 – Leukocyte (WBCs) content, RBCs Indexes and membrane protein senescence markers in cell density fractions enriched in young (Y) and senescent (S) RBCs separated from L- and N-RBCs units (n=4) during the storage.

	L-RBCs day 8		N-RBCs day8		L-RBCs day 36		N-RBCs day 36	
	Y-RBCs	S-RBCs	Y-RBCs	S-RBCs	Y-RBCs	S-RBCs	Y-RBCs	S-RBCs
WBCs ($\times 10^3/\mu L$)	0.2±0.0	0.2±0.0	0.2±0.0	n.d.[a]	n.d.[a]	0.1±0.0	0.1±0.1	0.1±0.0
MCV (fL)	98.6±2.2[§*]	82.1±1.8[§]	94.3±1.7[§*]	82.1±2.5[§]	96.8±2.3[§*]	85.9±1.7[§]	91.5±2.8[§*]	83.2±1.3[§]
MCH (pg)	29.4±0.5[§*]	31.3±0.3[§*]	27.9±0.8[*]	29.7±1.1[*]	30.3±0.3[§*]	32.1±0.5[§*]	26.8±1.4[§*]	30.3±0.9[§*]
MCHC (g/dL)	29.8±0.4[§]	38.1±0.5[§*]	29.5±0.3[§]	36.2±0.6[§*]	31.3±0.6[§*]	37.2±0.7[§]	29.3±0.5[§*]	36.4±0.6[§]
RDW-CV (%)	13.3±0.6	14.5±0.7	13.1±0.5	14.1±0.5	12.3±0.7	13.1±0.6	11.7±0.6	12.5±0.4
Spectrin-Hb complex[b]	1.0±0.2[§*]	17±1.8[§]	9.6±2.3[§*]	19.4±3.5[§]	64.8±9.2[§*]	103.5±16.7[§*]	97.8±12.3[§*]	188±25.6[§*]
Oxidized Hb[b]	1.0±0.2[§*]	2.4±0.4[*]	2.4±0.4[§*]	3.9±0.5[*]	5.6±0.8[§*]	8.9±1.1[*]	10.0±2.1[§*]	14.5±1.9[*]
Band 3 modifications[b]	1.0±0.2[§]	3.3±0.5[*]	1.0±0.3[§]	2.3±0.4[*]	4.9±0.9[§*]	11.9±1.8	9.7±1.5[§*]	15.8±2.5

Results are presented as mean±SD.
[a] Non-detected (less than detection limit).
[b] Normalization to the day 8 levels of L-RBCs.
[*] $p<0.05$ L-RBCs vs. N-RBCs.
[§] $p<0.05$ Y-RBCs vs. S-RBCs.

Fig. 7A–C, there was a constant trend for higher distortions levels in the non-leukoreduced Y-RBCs compared to the L-ones, that reached statistic significance on days 36 (calcium and PCI) or 42 (ROS) of storage. The stress phenotype was even more intently manifested at the membrane proteome level, namely in the variation of a range of aging and oxidative/calcium-associated markers, as those shown in Fig. 7D. Indeed, either during some period (band 3 modifications as well as membrane bound IgGs, calpain and Prx2), or during the whole storage time (spectrin-Hb cross-linking and binding of oxidized/denatured Hb to the membrane), the non-leukoreduced Y-RBCs were characterized by substantially higher expression of stress markers compared to the pre-storage leukoreduced Y-RBCs (Fig. 7D). The molecular chaperone HSP70 was also found significantly increased in the Y-RBCs of the non-leukoreduced units vs. the L-ones after prolonged storage (data not shown).

Aging is a complicated molecular process that involves strong interrelationships between the cells and their cellular and biochemical environment. *Ex vivo* storage of RBCs under various conditions is a model system for studying those effects. For instance, differential pattern of cellular senescence and response to oxidative stress has been found in RBCs stored with or without mannitol [17]. In the same context, RBCs aging-related events are expected to be differently influenced by the presence of contaminant leukocytes and platelets during the storage.

The excessive manifestation of aging and stress markers on membrane proteome is not a surprising finding, considering that the RBCs membrane is an unusually dynamic structure and a sensitive biosensor of cellular stress. Unlike the ROS and calcium measurements that performed on whole cell preparations, the membrane proteome analysis is more focused and as such, it probably reveals the targeted effect of ROS and calcium disturbances. For instance, the main, directly visible feature of the oxidatively altered RBCs is the accumulation of membrane-bound oxidized/denatured Hb that was found significantly elevated in the low-density N-RBCs. The cross linked Hb species bind to membrane and cytoskeleton targets such as band 3 and spectrin [4] to trigger a cascade of events affecting RBCs rigidity, echinocytosis, adherence, erythrophagocytosis as well as post transfusion survival of damaged RBCs [1,66,84]. Unlike cytosolic ROS, ROS generated in close proximity to the membrane after Hb binding, are not fully accessible to the cytosolic antioxidants and as such they might be especially active not only against local targets but also against nearby tissues and cells after their release from RBCs [94]. Considering that S-RBCs are not removed during the storage, their increased population in N-units [50] may therefore accelerate the *in vitro* aging process of stored RBCs.

In accordance with previous studies reporting increased *in vitro* phagocytosis of RBCs without prior leukodepletion [50], our findings imply that the vicinity with contaminant cells renders the young N-RBCs of the lower density fraction somehow older, injured and more stressed than their age-mate L-RBCs. This effect might be related to either higher stress imposition and/or to more severe diminution in RBCs antioxidant defense capacity [1,64]. Indeed, leukocytes- and platelets-derived enzymes, toxic reactive oxygen and nitrogen species might affect RBCs mechanical integrity and erythrophagocytosis by performing detrimental interactions with numerous RBCs components [11,36,53,67]. Considering that granulocytes disintegrate after 24 h [95], their fragments and released material may pass the filter and still contribute to secondary RBCs storage damage. Therefore, a proportion of the storage lesion seen in the L-RBCs might also be related to the donor leukocyte effects. Despite that, our results provide new evidence to support the notion that pre-storage leukoreduction effectively reduces RBCs damage caused by the residual leukocytes and platelets. Leukoreduction slows down the progression of the senescence process in stored RBCs, probably by alleviating the oxidative and calcium stress.

3.7. *The possible molecular and cellular effects of contaminant donor's cells on stored RBCs*

Although the donor's contaminant cells represent a scant minority compared to the predominant population of RBCs, their co-storage for 42 days in the cold might aggravate the RBCs structural and functional integrity through an array of detrimental intercellular interactions. We have to take into consideration that the majority of the leukocytes and platelets have significantly shorter lifespan compared to that of RBCs. Furthermore, platelets produced from whole blood donations are effectively stored for transfusion purposes for five days at 22 °C while neutrophils are not stored at all. Moreover, the storage unit represents a close system. In the absence of a clearance mechanism, the cells have to put up with their own and other cells wastes and by-products. The contaminant cells might affect RBCs through their metabolism, glucose consumption and release of a great variety of biologically active compounds (free radicals, extracellular vesicles, enzymes, cytokines etc.) that are restively produced after cellular activation, apoptosis or breakdown. Table 1 depicts a decrease in the absolute leukocytes and platelets number over storage time. Leukocytes apoptosis, first of granulocytes and then of lymphocytes, starts from the first 2–3 days of storage and results in the formation of biologic response modifiers and membrane fragments that can be adhered to stored RBCs initiating removal signaling cascades [52]. Cytokines are known to be involved in apoptosis, while neutrophils, by Fas ligand shedding, might mediate death signaling in the Fas-bearing lymphocytes and RBCs. Notably, cytoskeleton and band 3 modifications as well as PS externalization following the activation of the membrane-based apoptotic pathway have been reported in the past in both senescent and stored RBCs [3,17,96,97]. Leukocytes and activated platelets are important sources of free radicals and biologically effective molecules that are simply accumulated in the supernatants probably not as innocent bystanders but rather as effective mediators of RBCs senescence and cold storage stress. Reactive oxygen and nitrogen species as well as soluble enzymes hit directly the sensitive RBCs proteins, glyco-conjugates and membrane lipids while significant amounts of platelet- and leukocyte-derived extracellular membrane vesicles enhanced the toxicity of the storage supernatant. It has been reported that the ROS generated by human neutrophils are cytotoxic for RBCs via an Hb oxidation mechanism [67] that is the initiating event in some major RBCs senescent pathways. Moreover, the contaminant cells-derived proteases are expected to be more effective toward stored RBCs compared to the *in vivo* conditions because stored RBCs lack the protective effect of the protease

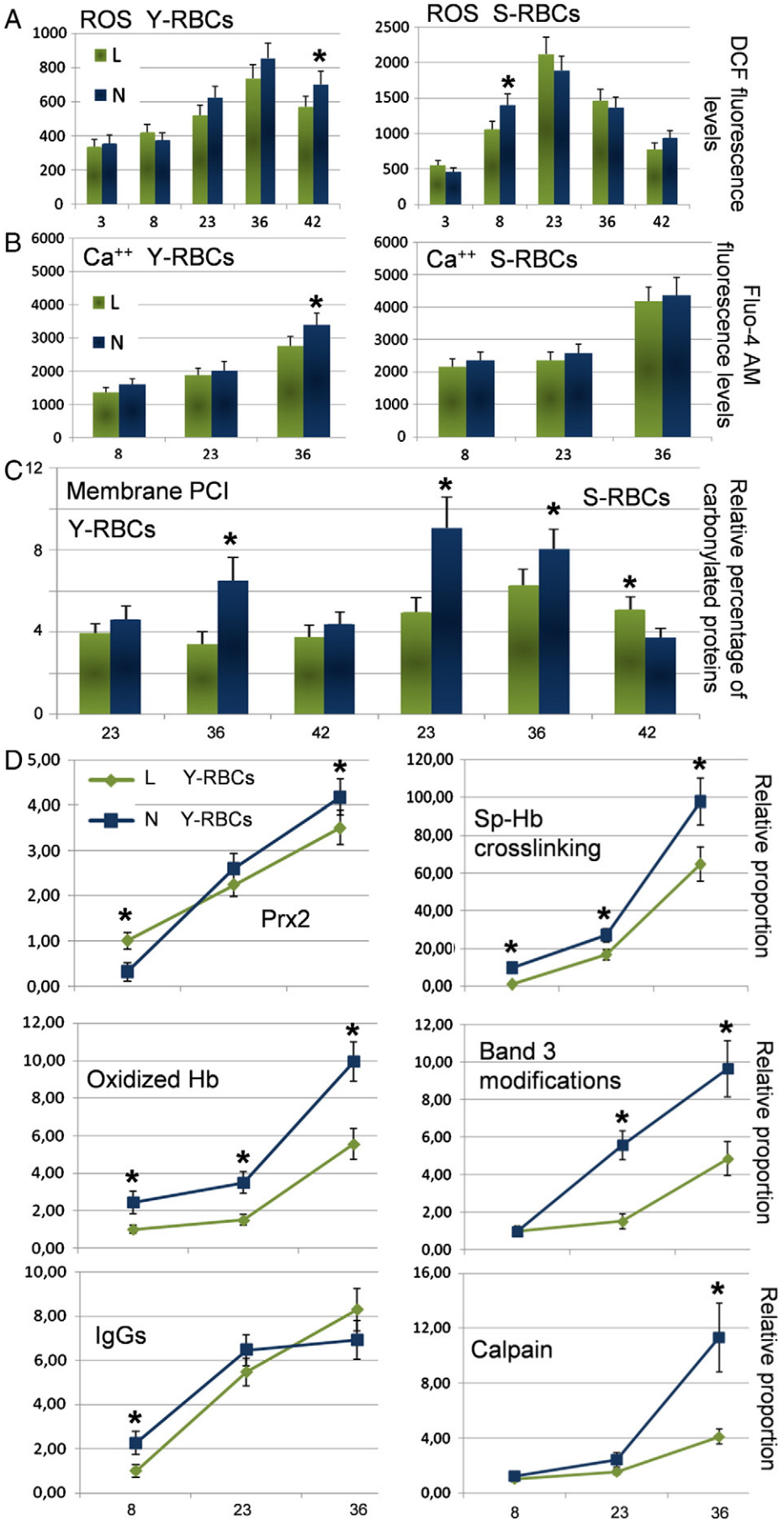
A
ROS Y-RBCs
ROS S-RBCs
L
N
DCF fluorescence levels
B
Ca++ Y-RBCs
Ca++ S-RBCs
Fluo-4 AM fluorescence levels
C
Membrane PCI
Y-RBCs
S-RBCs
Relative percentage of carbonylated proteins
D
L Y-RBCs
N Y-RBCs
Prx2
Sp-Hb crosslinking
Oxidized Hb
Band 3 modifications
IgGs
Calpain
Relative proportion

inhibitors-containing plasma [98]. In addition, the residual platelets experience a kind of "cold storage lesion" at the low temperature of the RBCs units, which apart from poor survival in the circulation, includes a type of activation state and relevant signaling via the plasma membrane: irreversible transformation, increase in intracellular calcium and protein tyrosine phosphorylation, lipid rafts aggregation, secretion of alpha granule and lysosomal contents, rearrangement of the surface glycoprotein Ib, P38MAPK and cytosolic phospholipase A2 activation, arachidonic acid release, apoptosis, PS externalization and accelerated membrane vesiculation [99–102]. Indeed, it has been reported that platelet-derived microparticles accumulate from day 0 and peak on day 20 of storage, while the leukocyte-derived vesicles are increased after the day 30 in stored non-leukoreduced RBCs units [103]. Pre-storage leukofiltration not only substantially reduces RBCs membrane vesiculation but also post-storage platelet-derived microparticles count [104]. The enrichment of supernatant in microvesicles under non-leukoreduction conditions leads to a sharp increase in the inter-cellular communication potential of the unit. The extracellular vesicles are potent packages of information since they contain numerous and highly concentrated signaling materials, including activated caspases and PS. As a result, they might exhibit pleiotropic stimulatory effects on cells via receptor interactions or direct transfer of their protein and lipid components by fusion with the cellular membrane [105], as previously reported for the RBCs-derived vesicles *in vivo* [106]. Consequently, the greater variability in extracellular vesicles released in N-RBCs is expected to effectively modify the signaling machinery of RBCs targets.

3.8. Conclusions

The present study provides further insight into the mechanisms of the RBC storage lesion in relation to the effect of pre-storage leukoreduction. Although storage lesion is usually enhanced in both L- and N-RBCs by prolonged storage, it is partially alleviated by filtering removal of the donor's contaminant leukocytes and platelets. Substantiated evidence comes from a series of different yet physiologically interlinked experimental data. L-RBCs excel N-RBCs at almost all the storage quality measurements examined, either for a part or for the whole of the storage period. Indeed, hemolysis, irreversible echinocytosis, microvesiculation, removal signaling, ROS and calcium accumulation, band 3-related senescence modifications, membrane proteome stress biomarkers as well as emergence of a senescence phenotype in the lower density RBCs that is disproportionate to their age, are all encountered more or mostly in N-RBCs compared to the L-ones. It seems that the residual leukocytes and platelets impose a great burden of oxidative and calcium-associated stress on RBCs that is reflected in the accumulation of more senescent defects. Although a direct connection between the elevated ROS and calcium levels with their triggering potential towards senescence and death signaling is missing in our study, the different storage lesion profile in relation to the presence or no of contaminant cells implies a significant degree of correlation. Probably through the early events of cellular activation, apoptosis and degeneration of the donor's leukocytes and platelets, a considerable fraction of the N-RBCs that are not yet physiologically senescent become damaged and more susceptible to the noxious effects of storage. The currently reported molecular and cellular data provide a mechanistic basis for the improved storage and post transfusion recovery seen in the case of pre-storage leukoreduction. Based on these results it will be interesting to evaluate the contaminant cells "cold storage lesion" in parallel to the RBCs defects during the storage period in order to assign specific roles in every participant of this clinically important cellular fellowship.

Acknowledgements

The authors wish to thank all blood donors that have participated in the present study, and especially the four friends that donated twice, for their prompt, volunteer response, and exceptional collaboration; the PhD student Georgatzakou H. and the pre-graduate students Taihert M. and Kollarou A. (Dept. of Cell Biology & Biophysics, Faculty of Biology, NKUA) for their assistance in the performance of a part of the immunoblotting experiments; and finally, Assistant Prof. I.P. Trougakos (Dept. of Cell Biology & Biophysics, Faculty of Biology, NKUA) for the kind disposal of fluorometer device. This study was partly supported by the "Special Account for Research Grants of the NKUA" to Associate Prof. I.S. Papassideri.

REFERENCES

[1] Lion N, Crettaz D, Rubin O, Tissot JD. Stored red blood cells: a changing universe waiting for its map(s). J Proteomics 2010;73:374–85.
[2] Antonelou MH, Kriebardis AG, Papassideri IS. Aging and death signalling in mature red cells: from basic science to transfusion practice. Blood Transfus 2010;8(Suppl. 3):s39–47.
[3] Kriebardis AG, Antonelou MH, Stamoulis KE, Economou-Petersen E, Margaritis LH, Papassideri IS. Storage-dependent remodeling of the red blood cell membrane is associated with increased immunoglobulin G binding, lipid raft rearrangement, and caspase activation. Transfusion 2007;47:1212–20.
[4] Kriebardis AG, Antonelou MH, Stamoulis KE, Economou-Petersen E, Margaritis LH, Papassideri IS. Progressive oxidation of cytoskeletal proteins and accumulation of denatured hemoglobin in stored red cells. J Cell Mol Med 2007;11:148–55.

Fig. 7 – Comparative analysis of young (Y) and senescent (S) RBCs of various storage periods separated from L- and N-units by Percoll density gradient fractionation. Averaged (n = 8) intracellular ROS (A) and calcium (B) accumulation as well as membrane PCI (C) analysis revealed a different variation profile not only between Y- and S-RBCs but also between L- and N-groups. (D) Graphs showing the averaged variation in a series of cellular aging and stress protein markers in low-density L- and N-RBCs collected at the indicated three time-points of storage. Error bars: SD; (*) $p < 0.05$ of L- vs. N-RBCs.

[5] Zimrin AB, Hess JR. Current issues relating to the transfusion of stored red blood cells. Vox Sang 2009;96:93–103.
[6] Card RT, Mohandas N, Mollison PL. Relationship of post-transfusion viability to deformability of stored red cells. Br J Haematol 1983;53:237–40.
[7] van de Watering L. Red cell storage and prognosis. Vox Sang 2011;100:36–45.
[8] Weinberg JA, McGwin Jr G, Griffin RL, Huynh VQ, Cherry III SA, Marques MB, et al. Age of transfused blood: an independent predictor of mortality despite universal leukoreduction. J Trauma 2008;65:279–82 discussion 82–4.
[9] Hess JR, Sparrow RL, van der Meer PF, Acker JP, Cardigan RA, Devine DV. Red blood cell hemolysis during blood bank storage: using national quality management data to answer basic scientific questions. Transfusion 2009;49:2599–603.
[10] Hess JR, Greenwalt TG. Storage of red blood cells: new approaches. Transfus Med Rev 2002;16:283–95.
[11] Racek J, Herynkova R, Holecek V, Faltysova J, Krejcova I. What is the source of free radicals causing hemolysis in stored blood? Physiol Res 2001;50:383–8.
[12] Baumgartner JM, Nydam TL, Clarke JH, Banerjee A, Silliman CC, McCarter MD. Red blood cell supernatant potentiates LPS-induced proinflammatory cytokine response from peripheral blood mononuclear cells. J Interferon Cytokine Res 2009;29:333–8.
[13] Sparrow RL. Red blood cell storage and transfusion-related immunomodulation. Blood Transfus 2010;8(Suppl. 3):s26–30.
[14] Heaton WA, Holme S, Smith K, Brecher ME, Pineda A, AuBuchon JP, et al. Effects of 3–5 log10 pre-storage leucocyte depletion on red cell storage and metabolism. Br J Haematol 1994;87:363–8.
[15] Ran Q, Hao P, Xiao Y, Zhao J, Ye X, Li Z. Effect of irradiation and/or leucocyte filtration on RBC storage lesions. PLoS One 2011;6:e18328.
[16] Grimshaw K, Sahler J, Spinelli SL, Phipps RP, Blumberg N. New frontiers in transfusion biology: identification and significance of mediators of morbidity and mortality in stored red blood cells. Transfusion 2011;51:874–80.
[17] Antonelou MH, Kriebardis AG, Stamoulis KE, Economou-Petersen E, Margaritis LH, Papassideri IS. Red blood cell aging markers during storage in citrate-phosphate-dextrose-saline-adenine-glucose-mannitol. Transfusion 2010;50:376–89.
[18] Zwart A, van Assendelft OW, Bull BS, England JM, Lewis SM, Zijlstra WG. Recommendations for reference method for haemoglobinometry in human blood (ICSH standard 1995) and specifications for international haemiglobinocyanide standard (4th edition). J Clin Pathol 1996;49:271–4.
[19] Sowemimo-Coker SO. Red blood cell hemolysis during processing. Transfus Med Rev 2002;16:46–60.
[20] Reinhart WH, Chien S. Red cell rheology in stomatocyte-echinocyte transformation: roles of cell geometry and cell shape. Blood 1986;67:1110–8.
[21] Antonelou MH, Kriebardis AG, Velentzas AD, Kokkalis AC, Georgakopoulou SC, Papassideri IS. Oxidative stress-associated shape transformation and membrane proteome remodeling in erythrocytes of end stage renal disease patients on hemodialysis. J Proteomics 2011;74:2441–52.
[22] Berezina TL, Zaets SB, Morgan C, Spillert CR, Kamiyama M, Spolarics Z, et al. Influence of storage on red blood cell rheological properties. J Surg Res 2002;102:6–12.
[23] D'Alessandro A, D'Amici GM, Vaglio S, Zolla L. Time-course investigation of SAGM-stored leukocyte-filtered red bood cell concentrates: from metabolism to proteomics. Haematologica 2012;97:107–15.
[24] Balzan S, D'Urso G, Nicolini G, Forini F, Pellegrino M, Montali U. Erythrocyte sodium pump stimulation by ouabain and an endogenous ouabain-like factor. Cell Biochem Funct 2007;25:297–303.
[25] Terra HT, Saad MJ, Carvalho CR, Vicentin DL, Costa FF, Saad ST. Increased tyrosine phosphorylation of band 3 in hemoglobinopathies. Am J Hematol 1998;58:224–30.
[26] Ferru E, Giger K, Pantaleo A, Campanella E, Grey J, Ritchie K, et al. Regulation of membrane-cytoskeletal interactions by tyrosine phosphorylation of erythrocyte band 3. Blood 2011;117:5998–6006.
[27] Bordin L, Ion-Popa F, Brunati AM, Clari G, Low PS. Effector-induced Syk-mediated phosphorylation in human erythrocytes. Biochim Biophys Acta 2005;1745:20–8.
[28] Bosch FH, Werre JM, Roerdinkholder-Stoelwinder B, Huls TH, Willekens FL, Halie MR. Characteristics of red blood cell populations fractionated with a combination of counterflow centrifugation and Percoll separation. Blood 1992;79:254–60.
[29] Antonelou MH, Kriebardis AG, Stamoulis KE, Trougakos IP, Papassideri IS. Apolipoprotein J/Clusterin is a novel structural component of human erythrocytes and a biomarker of cellular stress and senescence. PLoS One 2011;6:e26032.
[30] Greenwalt TJ, Dumaswala UJ. Effect of red cell age on vesiculation *in vitro*. Br J Haematol 1988;68:465–7.
[31] Kriebardis AG, Antonelou MH, Stamoulis KE, Economou-Petersen E, Margaritis LH, Papassideri IS. RBC-derived vesicles during storage: ultrastructure, protein composition, oxidation, and signaling components. Transfusion 2008;48:1943–53.
[32] Beutler E, West C, Blume KG. The removal of leukocytes and platelets from whole blood. J Lab Clin Med 1976;88:328–33.
[33] Henkelman S, Dijkstra-Tiekstra MJ, de Wildt-Eggen J, Graaff R, Rakhorst G, van Oeveren W. Is red blood cell rheology preserved during routine blood bank storage? Transfusion 2010;50:941–8.
[34] Hess JR. Red cell changes during storage. Transfus Apher Sci 2010;43:51–9.
[35] Haradin AR, Weed RI, Reed CF. Changes in physical properties of stored erythrocytes relationship to survival in vivo. Transfusion 1969;9:229–37.
[36] Greenwalt TJ, Zehner Sostok C, Dumaswala UJ. Studies in red blood cell preservation. 1. Effect of the other formed elements. Vox Sang 1990;58:85–9.
[37] Willekens FL, Werre JM, Groenen-Dopp YA, Roerdinkholder-Stoelwinder B, de Pauw B, Bosman GJ. Erythrocyte vesiculation: a self-protective mechanism? Br J Haematol 2008;141:549–56.
[38] Bosman GJ, Werre JM, Willekens FL, Novotny VM. Erythrocyte ageing *in vivo* and *in vitro*: structural aspects and implications for transfusion. Transfus Med 2008;18:335–47.
[39] Dumaswala UJ, Dumaswala RU, Levin DS, Greenwalt TJ. Improved red blood cell preservation correlates with decreased loss of bands 3, 4.1, acetylcholinestrase, and lipids in microvesicles. Blood 1996;87:1612–6.
[40] Tinmouth A, Chin-Yee I. The clinical consequences of the red cell storage lesion. Transfus Med Rev 2001;15:91–107.
[41] Wagner GM, Chiu DT, Qju JH, Heath RH, Lubin BH. Spectrin oxidation correlates with membrane vesiculation in stored RBCs. Blood 1987;69:1777–81.
[42] Tait JF, Gibson D. Measurement of membrane phospholipid asymmetry in normal and sickle-cell erythrocytes by means of annexin V binding. J Lab Clin Med 1994;123:741–8.
[43] Lu C, Shi J, Yu H, Hou J, Zhou J. Procoagulant activity of long-term stored red blood cells due to phosphatidylserine exposure. Transfus Med 2011;21:150–7.
[44] Bosman GJ, Cluitmans JC, Groenen YA, Werre JM, Willekens FL, Novotny VM. Susceptibility to hyperosmotic stress-induced phosphatidylserine exposure increases during red blood cell storage. Transfusion 2011;51:1072–8.

[45] Boas FE, Forman L, Beutler E. Phosphatidylserine exposure and red cell viability in red cell aging and in hemolytic anemia. Proc Natl Acad Sci U S A 1998;95:3077–81.
[46] Verhoeven AJ, Hilarius PM, Dekkers DW, Lagerberg JW, de Korte D. Prolonged storage of red blood cells affects aminophospholipid translocase activity. Vox Sang 2006;91: 244–51.
[47] Geldwerth D, Kuypers FA, Butikofer P, Allary M, Lubin BH, Devaux PF. Transbilayer mobility and distribution of red cell phospholipids during storage. J Clin Invest 1993;92: 308–14.
[48] Stewart A, Urbaniak S, Turner M, Bessos H. The application of a new quantitative assay for the monitoring of integrin-associated protein CD47 on red blood cells during storage and comparison with the expression of CD47 and phosphatidylserine with flow cytometry. Transfusion 2005;45:1496–503.
[49] Sparrow RL, Healey G, Patton KA, Veale MF. Red blood cell age determines the impact of storage and leukocyte burden on cell adhesion molecules, glycophorin A and the release of annexin V. Transfus Apher Sci 2006;34:15–23.
[50] Bratosin D, Leszczynski S, Sartiaux C, Fontaine O, Descamps J, Huart JJ, et al. Improved storage of erythrocytes by prior leukodepletion: flow cytometric evaluation of stored erythrocytes. Cytometry 2001;46:351–6.
[51] Cardo LJ, Hmel P, Wilder D. Stored packed red blood cells contain a procoagulant phospholipid reducible by leukodepletion filters and washing. Transfus Apher Sci 2008;38:141–7.
[52] Frabetti F, Musiani D, Marini M, Fanelli C, Coppola S, Ghibelli L, et al. White cell apoptosis in packed red cells. Transfusion 1998;38:1082–9.
[53] Hogman CF, Meryman HT. Storage parameters affecting red blood cell survival and function after transfusion. Transfus Med Rev 1999;13:275–96.
[54] Luk CS, Gray-Statchuk LA, Cepinkas G, Chin-Yee IH. WBC reduction reduces storage-associated RBC adhesion to human vascular endothelial cells under conditions of continuous flow *in vitro*. Transfusion 2003;43:151–6.
[55] Romero PJ, Romero EA. The role of calcium metabolism in human red blood cell ageing: a proposal. Blood Cells Mol Dis 1999;25:9–19.
[56] Palek J, Stewart G, Lionetti FJ. The dependence of shape of human erythrocyte ghosts on calcium, magnesium, and adenosine triphosphate. Blood 1974;44:583–97.
[57] Kiefer CR, Snyder LM. Oxidation and erythrocyte senescence. Curr Opin Hematol 2000;7:113–6.
[58] Wolfe LC. The membrane and the lesions of storage in preserved red cells. Transfusion 1985;25: 185–203.
[59] Bennett-Guerrero E, Veldman TH, Doctor A, Telen MJ, Ortel TL, Reid TS, et al. Evolution of adverse changes in stored RBCs. Proc Natl Acad Sci U S A 2007;104:17063–8.
[60] Salamino F, Sparatore B, Melloni E, Michetti M, Viotti PL, Pontremoli S, et al. The plasma membrane calcium pump is the preferred calpain substrate within the erythrocyte. Cell Calcium 1994;15:28–35.
[61] Kanias T, Acker JP. Mechanism of hemoglobin-induced cellular injury in desiccated red blood cells. Free Radic Biol Med 2010;49:539–47.
[62] Gottlieb Y, Topaz O, Cohen LA, Yakov LD, Haber T, Morgenstern A. Physiologically aged red blood cells undergo erythrophagocytosis *in vivo* but not *in vitro*. Haematologica 2012;97:994–1035.
[63] Kanias T, Acker JP. Biopreservation of red blood cells–the struggle with hemoglobin oxidation. FEBS J 2010;277:343–56.
[64] Jozwik M, Szczypka M, Gajewska J, Laskowska-Klita T. Antioxidant defence of red blood cells and plasma in stored human blood. Clin Chim Acta 1997;267:129–42.
[65] Messana I, Ferroni L, Misiti F, Girelli G, Pupella S, Castagnola M, et al. Blood bank conditions and RBCs: the progressive loss of metabolic modulation. Transfusion 2000;40:353–60.
[66] Lachant NA, Noble NA, Myrhe BA, Tanaka KR. Antioxidant metabolism during blood storage and its relationship to posttransfusion red cell survival. Am J Hematol 1984;17: 237–49.
[67] Weiss SJ. The role of superoxide in the destruction of erythrocyte targets by human neutrophils. J Biol Chem 1980;255:9912–7.
[68] Pietersz RN, Reesink HW, de Korte D, Dekker WJ, van den Ende A, Loos JA. Storage of leukocyte-poor red cell concentrates: filtration in a closed system using a sterile connection device. Vox Sang 1989;57:29–36.
[69] Chin-Yee I, Keeney M, Krueger L, Dietz G, Moses G. Supernatant from stored red cells activates neutrophils. Transfus Med 1998;8:49–56.
[70] Pantaleo A, Ferru E, Giribaldi G, Mannu F, Carta F, Matte A, et al. Oxidized and poorly glycosylated band 3 is selectively phosphorylated by Syk kinase to form large membrane clusters in normal and G6PD-deficient red blood cells. Biochem J 2009;418:359–67.
[71] Low PS, Waugh SM, Zinke K, Drenckhahn D. The role of hemoglobin denaturation and band 3 clustering in red blood cell aging. Science 1985;227:531–3.
[72] Minetti G, Piccinini G, Balduini C, Seppi C, Brovelli A. Tyrosine phosphorylation of band 3 protein in Ca2+/A23187-treated human erythrocytes. Biochem J 1996;320(Pt 2):445–50.
[73] Turrini F, Arese P, Yuan J, Low PS. Clustering of integral membrane proteins of the human erythrocyte membrane stimulates autologous IgG binding, complement deposition, and phagocytosis. J Biol Chem 1991;266:23611–7.
[74] Kriebardis AG, Antonelou MH, Stamoulis KE, Economou-Petersen E, Margaritis LH, Papassideri IS. Membrane protein carbonylation in non-leukodepleted CPDA-preserved red blood cells. Blood Cells Mol Dis 2006;36:279–82.
[75] Bosman GJ, Lasonder E, Luten M, Roerdinkholder-Stoelwinder B, Novotny VM, Bos H, et al. The proteome of red cell membranes and vesicles during storage in blood bank conditions. Transfusion 2008;48: 827–35.
[76] Rinalducci S, D'Amici GM, Blasi B, Vaglio S, Grazzini G, Zolla L. Peroxiredoxin-2 as a candidate biomarker to test oxidative stress levels of stored red blood cells under blood bank conditions. Transfusion 2011;51:1439–49.
[77] Rocha S, Vitorino RM, Lemos-Amado FM, Castro EB, Rocha-Pereira P, Barbot J, et al. Presence of cytosolic peroxiredoxin 2 in the erythrocyte membrane of patients with hereditary spherocytosis. Blood Cells Mol Dis 2008;41:5–9.
[78] Low FM, Hampton MB, Winterbourn CC. Peroxiredoxin 2 and peroxide metabolism in the erythrocyte. Antioxid Redox Signal 2008;10:1621–30.
[79] Stuhlmeier KM, Kao JJ, Wallbrandt P, Lindberg M, Hammarstrom B, Broell H, et al. Antioxidant protein 2 prevents methemoglobin formation in erythrocyte hemolysates. Eur J Biochem 2003;270:334–41.
[80] Moore RB, Shriver SK. Protein 7.2b of human erythrocyte membranes binds to calpromotin. Biochem Biophys Res Commun 1997;232:294–7.
[81] D'Amici GM, Rinalducci S, Zolla L. Proteomic analysis of RBC membrane protein degradation during blood storage. J Proteome Res 2007;6:3242–55.
[82] Ando K, Beppu M, Kikugawa K, Hamasaki N. Increased susceptibility of stored erythrocytes to anti-band 3 IgG autoantibody binding. Biochim Biophys Acta 1993;1178:127–34.
[83] Snyder LM, Leb L, Piotrowski J, Sauberman N, Liu SC, Fortier NL. Irreversible spectrin-haemoglobin crosslinking in vivo: a marker for red cell senescence. Br J Haematol 1983;53:379–84.

[84] Snyder LM, Fortier NL, Trainor J, Jacobs J, Leb L, Lubin B, et al. Effect of hydrogen peroxide exposure on normal human erythrocyte deformability, morphology, surface characteristics, and spectrin-hemoglobin cross-linking. J Clin Invest 1985;76:1971–7.
[85] Salzer U, Hinterdorfer P, Hunger U, Borken C, Prohaska R. Ca(++)-dependent vesicle release from erythrocytes involves stomatin-specific lipid rafts, synexin (annexin VII), and sorcin. Blood 2002;99:2569–77.
[86] Glaser T, Schwarz-Benmeir N, Barnoy S, Barak S, Eshhar Z, Kosower NS. Calpain (Ca(2+)-dependent thiol protease) in erythrocytes of young and old individuals. Proc Natl Acad Sci U S A 1994;91:7879–83.
[87] Antonelou MH, Kriebardis AG, Stamoulis KE, Trougakos IP, Papassideri IS. Apolipoprotein J/clusterin in human erythrocytes is involved in the molecular process of defected material disposal during vesiculation. PLoS One 2011;6:e26033.
[88] Anniss AM, Sparrow RL. Expression of CD47 (integrin-associated protein) decreases on red blood cells during storage. Transfus Apher Sci 2002;27:233–8.
[89] Long KE, Yomtovian R, Kida M, Knez JJ, Medof ME. Time-dependent loss of surface complement regulatory activity during storage of donor blood. Transfusion 1993;33:294–300.
[90] Goodman SR, Kurdia A, Ammann L, Kakhniashvili D, Daescu O. The human red blood cell proteome and interactome. Exp Biol Med (Maywood) 2007;232:1391–408.
[91] Bosch FH, Werre JM, Schipper L, Roerdinkholder-Stoelwinder B, Huls T, Willekens FL, et al. Determinants of red blood cell deformability in relation to cell age. Eur J Haematol 1994;52:35–41.
[92] Romero PJ, Romero EA, Winkler MD. Ionic calcium content of light dense human red cells separated by Percoll density gradients. Biochim Biophys Acta 1997;1323:23–8.
[93] Shiga T, Sekiya M, Maeda N, Kon K, Okazaki M. Cell age-dependent changes in deformability and calcium accumulation of human erythrocytes. Biochim Biophys Acta 1985;814:289–99.
[94] Nagababu E, Mohanty JG, Bhamidipaty S, Ostera GR, Rifkind JM. Role of the membrane in the formation of heme degradation products in red blood cells. Life Sci 2010;86:133–8.
[95] Humbert JR, Fermin CD, Winsor EL. Early damage to granulocytes during storage. Semin Hematol 1991;28:10–3.
[96] Mandal D, Baudin-Creuza V, Bhattacharyya A, Pathak S, Delaunay J, Kundu M, et al. Caspase 3-mediated proteolysis of the N-terminal cytoplasmic domain of the human erythroid anion exchanger 1 (band 3). J Biol Chem 2003;278:52551–8.
[97] Mandal D, Mazumder A, Das P, Kundu M, Basu J. Fas-, caspase 8-, and caspase 3-dependent signaling regulates the activity of the aminophospholipid translocase and phosphatidylserine externalization in human erythrocytes. J Biol Chem 2005;280:39460–7.
[98] Bocci V, Pessina GP, Paulesu L. Studies of factors regulating the ageing of human erythrocytes-IV. Influence of physiological proteinase inhibitors. Int J Biochem 1981;13:1257–60.
[99] Egidi MG, D'Alessandro A, Mandarello G, Zolla L. Troubleshooting in platelet storage temperature and new perspectives through proteomics. Blood Transfus 2010;8(Suppl. 3):s73–81.
[100] Kaufman RM. Uncommon cold: could 4 degrees C storage improve platelet function? Transfusion 2005;45:1407–12.
[101] van derWal DE, Gitz E, Du VX, Lo KS, Koekman CA, Versteeg S, et al. Arachidonic acid depletion extends survival of cold stored platelets by interfering with [Glycoprotein Ibalpha - 14-3-3zeta] association. Haematologica in press. http://dx.doi.org/10.3324/haematol.2011.059956.
[102] Bode AP, Knupp CL. Effect of cold storage on platelet glycoprotein Ib and vesiculation. Transfusion 1994;34:690–6.
[103] Jy W, Ricci M, Shariatmadar S, Gomez-Marin O, Horstman LH, Ahn YS. Microparticles in stored red blood cells as potential mediators of transfusion complications. Transfusion 2011;51:886–93.
[104] Sugawara A, Nollet KE, Yajima K, Saito S, Ohto H. Preventing platelet-derived microparticle formation–and possible side effects-with prestorage leukofiltration of whole blood. Arch Pathol Lab Med 2010;134:771–5.
[105] Mause SF, Weber C. Microparticles: protagonists of a novel communication network for intercellular information exchange. Circ Res 2010;107:1047–57.
[106] Sloand EM, Mainwaring L, Keyvanfar K, Chen J, Maciejewski J, Klein HG, et al. Transfer of glycosylphosphatidylinositol-anchored proteins to deficient cells after erythrocyte transfusion in paroxysmal nocturnal hemoglobinuria. Blood 2004;104:3782–8.